ROLE OF PLATELET-DERIVED GROWTH FACTOR-ELASTIN LIKE POLYPEPTIDE IN CHRONIC WOUND HEALING

by

MEHMA KAUR CHAWLA

A Thesis submitted to the

School of Graduate Studies

Rutgers, The State University of New Jersey

In partial fulfillment of the requirements

For the degree of

Master of Science

Graduate Program in Biomedical Engineering

Written under the direction of

Dr. Francois Berthiaume and

Dr. Suneel Kumar

And approved by

_____

_____

_____

New Brunswick, New Jersey

October 2020

ABSTRACT OF THE THESIS

ROLE OF PLATELET DERIVED GROWTH FACTOR- ELASTIN LIKE POLYPEPTIDE (PDGF-ELP) FOR CHRONIC WOUND HEALING

By **MEHMA KAUR CHAWLA**

Thesis Director: Dr. Francois Berthiaume, PhD and Dr. Suneel Kumar, PhD

Chronic wounds are characterized as non-healing wounds due to poor angiogenesis, impaired vascularization, collagen formation, and dysfunctional fibroblasts and keratinocytes in the hypoxic wound environment. Recent studies have demonstrated the use of growth factors for enhanced wound healing due to their ability to promote proliferation and migration of cells, stimulate collagen synthesis and augment angiogenesis. Platelet-derived growth factor (PDGF) is one of the earliest growth factors to be identified and clinically used for the treatment of chronic wounds. However, their applications are limited because of the increased level of proteases in the hostile wound environment which degrades the growth factors, thus impeding their activity. Here, we have developed and characterized a recombinant fusion protein comprising PDGF and elastin-like polypeptide (ELP). The phase transitioning property of ELP allows rapid purification of the fusion protein using inverse temperature cycling (ITC). The fusion protein retained all characteristics of PDGF-A as evident from fibroblast and endothelial cell proliferation and migration, and endothelial formation of a tube network similar to native PDGF. The self-assembling property of ELP caused the formation of nanoparticles at physiological temperature, which acted as an optimal and stable delivery mechanism for the wound environment. We used 5 nM concentration of PDGF-ELP to show an

increase in proliferation by ~2 fold, ~90% wound closure after 48 hours using cell-based scratch assays, and increased angiogenesis demonstrated by enhanced capillary-like tube network formation using a tube assay.

ACKNOWLEDGEMENTS

I would like to thank several people who have supported me during my time at Rutgers and helped me towards my thesis work and degree completion. Dr. Berthiaume, thank you for agreeing to take me in your lab and guiding me along the way not only for my thesis project but also towards my career path. I would like to thank Dr. Suneel Kumar for training me in the lab and explaining important concepts and procedures that helped me perform the experiments successfully. I would also like to thank Dr. Rene Schloss for agreeing to be a part of my thesis defense as a committee member and providing comments that helped me work on my project and thesis writing.

Thank you Dr. Yarmush, for providing constructive comments during team meetings. I would also like to express my gratitude towards Amulya Veldanda for being a supportive friend and labmate. Outside my lab, I would like to thank Dr. Rick Cohen for the design construction of PDGF-ELP and providing expertise and suggestions in protein expression and purification. I want to take this opportunity to also thank all the members of the Yarmush and Berthiaume labs for their constant support and encouraging words that got me where I am today. Outside my Rutgers community, I would like to thank all my family members, friends, and roommates for cheering me up during difficult times and also being by my side. Mom and dad, thank you for your constant support and believing in me and my dreams. This work is partially supported by the New Jersey Commission on Spinal Cord Research and the U.S. Department of Defense.

TABLE OF CONTENT

List of Figures

List of Tables

CHAPTER 1: INTRODUCTION

1.1 CHRONIC WOUNDS

Chronic wounds, especially lower extremity ulcers pose a major challenge to patients and healthcare professionals. More than 5.7 million suffer from chronic leg and foot ulcers, alone in the U.S., which costs approximately $20 million per year [1]. Chronic ulcers occur mostly in patients suffering from diabetes and vascular disease leading to diabetic ulcers, pressure ulcers, and venous ulcers. This is accompanied by loss of function, higher morbidity, increased rate of recurrence, and impaired quality of life [2]. Around 10-15% of people suffering from diabetes mellitus develop foot ulcers [3]. Of this, 15-25% get their lower limb amputated, with a 50-60 % mortality rate recorded during the first 5 years post-amputation [4,5]. An estimated 0.2-1 % of the population in the U.S. suffer from venous foot ulcers [6]. Thus, chronic wounds are a significant burden due to the high costs of treatment, the frustration of the patients, and a major health and economic issue.

Chronic wounds are non-healing wounds that get arrested in the initial phases of wound healing and are unable to progress towards complete closure of the wounds [7]. In a normal acute wound, distinct but overlapping phases define the cellular and biochemical events in the wound microenvironment [8]. The first phase is the hemostasis/inflammatory phase that is characterized by platelet aggregation, removal of necrotic tissue, an influx of neutrophils, and activation of fibroblasts. The proliferation stage aims to reduce the affected area through keratinocyte activation, angiogenesis, and re-epithelialization, which may take up to 2 weeks. The final

remodeling phase starts 2-3 weeks after lesion formation which is defined by formation and reorganization of extracellular matrix and synthesis of collagen for maximum tensile strength of healed tissue [9, 10].

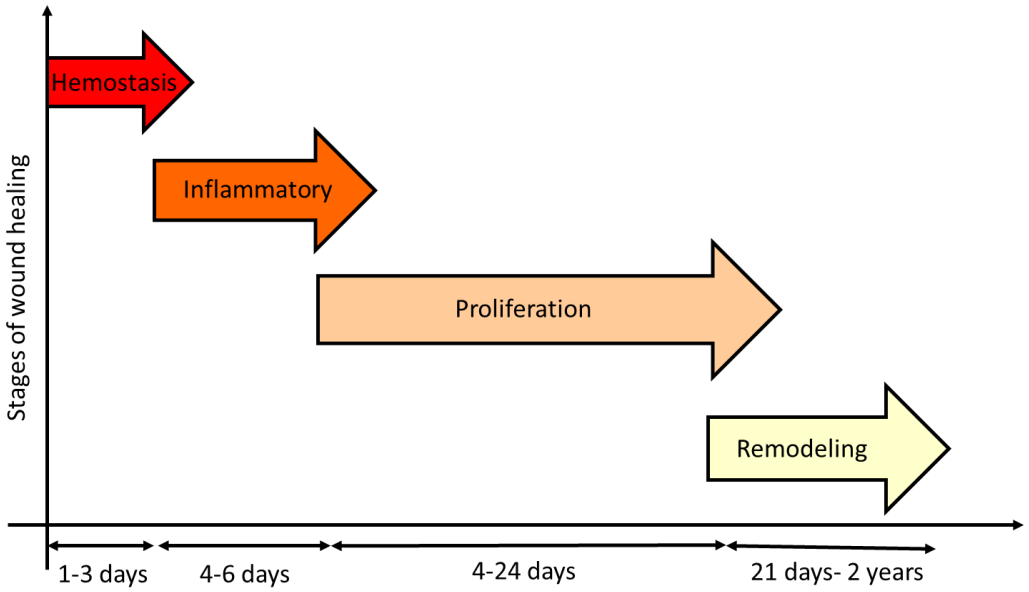

Figure 1.1: Phases of wound healing in an acute wound [8].

In contrast, the inflammatory phase in chronic wounds causes continuous activation of neutrophils throughout the healing process [7], resulting in further inflammation and upregulation of matrix metalloproteases (MMP) [11]. Higher levels of MMP cause abnormal degradation of the growth factors, negatively affecting the mitogenic activity of fibroblasts. Fibroblasts and keratinocytes become non-receptive to cytokines and reduced levels of growth factors, ultimately hindering ECM formation [12]. Insufficient angiogenesis and perfusion resulting from sensory neuropathy in diabetic condition cause hypoxia thereby prolonging the injury in the inflammatory phase [13, 14]. Impaired angiogenesis and vascularization, fibroblast and keratinocyte dysfunction,

hypoxia, reduced level of growth factors, and excessive protease activity contribute to impaired wound healing in the chronic wound environment [15].

1.2 AVAILABLE TREATMENTS

As evident from the above discussion, multiple factors contribute to the etiology of chronic wounds which makes it a complex problem to treat. The first most important therapeutic step is the removal of necrotic tissue. This process is called debridement and the dead tissue can be both surgically and enzymatically removed [16]. A common preventive treatment of chronic wounds is the topical application of antibacterial ointment at the site of injury [17]. Silver has been a popular ingredient in wound care products for almost 2000 years [18]. However, routine administration of these ointments does not always lead to better outcomes. Recent advances focus on integrating wound dressings like foam or hydrocolloid with antimicrobial agents like silver and betaine [19]. Offloading, negative pressure devices, the hyperbaric oxygen chamber, and the use of growth factors are some of the therapies that show promise in the treatment of non-healing wounds [20]. Despite reports of improved healing rates, there are several limitations to these methods that have been summarized in the table below:

Chronic wound treatment	Method	Disadvantages
Surgical debridement	Callus, non-viable soft tissue and bone removal using scalpel, nippers, and scissors	• Requires skill • Reoccurrence of ulcer
Enzymatic Debridement	Treatment available in the UK contains Streptokinase and Streptodornase. The treatment digests fibrin, collagen, and elastin found in the wound	• Contraindicated in patients with a risk of myocardial infarction • Expensive
Total Contact Cast (TCC)	Pressure relief and offloading	• Need for expertise • Skin irritation
Hyperbaric oxygen chamber	Increased supply of oxygen to tissue leading to improved angiogenesis and fibroblast proliferation	• Expensive • Not a substitute for other therapies
Negative pressure wound therapy	Latex-free foam airtight dressing with a negative pressure of 80-120 mmHg	• Not a replacement for surgical debridement • Higher material expenses
Growth factors	Topical application	• Limited bioavailability • Repeated application • Cost of treatment • Tumorigenicity

Table 1.1: Available chronic wound treatments and their limitations [16, 17, 18, 20].

1.3 GROWTH FACTORS

Growth factors are responsible for recruiting different cell types, promoting cell proliferation and migration, angiogenesis, and synthesis of collagen in the wound environment [21]. In a dysregulated wound environment, there is perturbation of

growth factors like transforming growth factor β (TGF-β), keratinocyte growth factor (KGF), epidermal growth factor (EGF), vascular endothelial growth factor (VEGF), basic fibroblast growth factor (b-FGF), platelet-derived growth factor (PDGF) and several other growth factors and cytokines. Thus, significant attention has been received for the exogenous application of one or a combination of these factors to enhance the healing process. The growth factor ligands bind to their specific receptors activating a cascade of molecular events leading to improved angiogenesis, re-epithelialization, granulation tissue formation, matrix formation, and the infiltration of the wound site by mesenchymal and endothelial cells [22]. Several recent studies have demonstrated accelerated wound closure by using co-delivery systems and a combination of growth factors with biomaterials [23, 24].

The acceptance of growth factors has not been as dramatic as hoped mostly due to the costs associated with the medication. Becaplermin gel is the only commercially available FDA approved growth factor (rhPDGF) [25]. There is also difficultly in interpreting clinical data from the use of becaplermin as different animal models respond differently to the treatment and the variability in wound closure rates in patients may demonstrate contradicting results in the efficacy of the gel [26]. More information and limitations on the use of growth factors have been highlighted in the following section.

1.4 PDGF FOR CHRONIC WOUNDS

There are five different isoforms of PDGF: PDGF AA, BB, CC, and DD are homodimers, whereas PDGF AB is a heterodimer[30]. PDGF A and B are ~100 amino acid long and

share a 60% sequence identity. PDGF-AA and BB are processed intracellularly whereas PDGF-CC, and DD are latent ligands and are not studied extensively[30]. PDGFs belong to a family of cystine knot type growth factors and bind to receptors PDGFα and PDGFβ that are a part of class III receptor tyrosine kinase (RTK). PDGF-A and PDGF-B consist of four anti-parallel β strands that are connected by disulfide bridges [30]. PDGFα is activated by binding with PDGF-AA, and PDGF-BB, whereas PDGF-β is activated by binding with PDGF-BB. PDGF-AB binds with both receptors [30].

PDGF was purified from platelets as early as 1979 [27]. They are found in all four stages of wound healing and are secreted by platelets, fibroblasts, keratinocytes, macrophages, and endothelial cells [28]. PDGF promotes mitogenic and chemotactic activity in fibroblasts, smooth muscle cells as well as regulates cell growth and division in endothelial cells [29]. Research has shown that PDGF might amplify angiogenesis and enhance endothelial cell proliferation *in vitro* [31]. *In vivo* experiments demonstrate that the growth factor supports blood vessel formation and maturation by recruiting pericytes to capillaries [32]. Under hypoxic conditions, PDGF upregulates the expression of VEGF in rabbit smooth muscle cells [33]. By enhancing fibroblast proliferation, PDGF targets tissue regeneration by increasing ECM formation [34].

Recombinant PDGF-BB is the growth factor for diabetic foot ulcer approved by the FDA and available in the market for clinical use. Pierce et al. showed that PDGF application improves the proliferative effect and formation of granulation tissue in rat incisional wound models [35, 36]. Significantly greater wound closure was observed in impaired wound healing model of genetically diabetic mice upon application of the growth factor

[37]. These pre-clinical studies showed promising results and was followed by human clinical trials for investigating the role of PDGF on chronic wound healing [38].

Becaplermin is the active ingredient in Regranex (rhPDGF-BB) which is based in sodium carboxymethylcellulose. Multicenter prospective randomized control trials were conducted to study the efficacy of the drug on diabetic foot ulcers [39]. The trials continued for 20 weeks and were followed-up 3 months after the end of each study. Phase II trial reported statistically significant wound healing in PDGF (30 μg/g) treated group vs the placebo group in 20 weeks (48 % vs 25 %) [39]. However, a Phase III study with 30 μg/g Becaplermin and placebo did not yield statistically significant data. The 100 μg/g Becaplermin group, however, showed a 50 % increase in wound closure rate as compared to the statistically lower 35% wound closure by placebo [40]. Another smaller study comparing 100 μg/g of Becaplermin and good ulcer care alone demonstrated a statistically insignificant difference in complete wound closure between the two groups (36 % vs 32 %, respectively) [41].

1.5 LIMITATIONS OF GROWTH FACTORS

Like many growth factors, PDGF is not very stable in the wound microfluid. The presence of several proteases makes it a hostile environment, thus degrading both endogenous and exogenously applied PDGF, which has a half-life in the order of hours [42]. The outermost skin layer poses difficultly in the permeation of topically administered growth factors, which are rapidly cleared from the wound bed, thus limiting their efficacy. Without an engineered delivery system, continuous application of the growth factor

makes it a costly and impractical therapeutic agent. Thus, a novel delivery system that facilitates sustained release and mitigates proteolysis is required for the stabilization of the protein [43].

The effectiveness of Becalpermin is still debatable due to the baseline variability in the complete wound closure of diabetic wounds in patients. Another consideration is the durability of the treatment, as only a 3-month follow-up study after 20 weeks of the trial was conducted. Recurrence rate was found to be 28% in all groups of treatment [39]. Overactivity of PDGF BB has been related to malignancies [44, 45]. FDA released a warning stating that increased rates of malignancies were observed in patients treated with 3 or more tubes of Regranex [46]. Cost-effectiveness is another criterion that needs to be looked into. Each 0.01 % Regranex tube costs about $1200, which needs to be applied twice daily for at least 20 weeks. This puts an economic burden on the patient suffering from diabetic chronic wounds.

1.6 PLATELET DERIVED GROWTH FACTOR- ELASTIN LIKE POLYPEPTIDE (PDGF-ELP) FUSION PROTEIN

Elastin like polypeptides (ELP) are repeats of Valine-Proline-Glycine-Xaa-Glycine, where X can be any naturally occurring amino acid except proline [78]. In our experiments we use pentapeptide repeats of ELP. Properties that make it useful for biomedical applications are its non-immunogenicity, non-pyrogenicity, and biocompatibility [47]. ELP can undergo a phase transition at physiological temperatures. Inverse temperature cycling (ITC) is used for purification of the fusion protein to high homogeneity without

the use of costly protein purification techniques [48]. Below the inverse transition temperature, the recombinant ELPs are soluble in aqueous solutions and above the transition temperature, they aggregate into self-assembling insoluble nanoparticles [49, 50].

By acting like “drug depots” they allow sustained release of the fusion protein over an extended time [51]. Recombinant ELP based proteins have also been shown to protect biomolecules from the proteolytic environment of the wound fluid by the formation of nanoparticles [52]. Senior et al. and Kamoun et al. demonstrated that elastin derived peptides also exhibit a role in dermal remodeling and regeneration by acting as mitogenic and chemotactic agents for fibroblasts [53, 54]. However, the role of ELP in cell proliferation and migration is still debatable.

Hence, we fabricated a fusion protein consisting of PDGF-A and ELP that has been shown to have the individual properties of both PDGF and ELP and may address some of the above-mentioned limitations of native PDGF in wound healing. We hypothesize that the recombinant fusion protein enhances cell proliferation, migration, and angiogenesis and therefore accelerates wound closure.

CHAPTER 2: PURIFICATION AND CHARACTERIZATION OF PDGF-ELP

2.1 INTRODUCTION

As discussed above, ELP tagged proteins have desirable effects in terms of purification, safety, biocompatibility, and dermal remodeling. In this section, we have discussed the transformation of the vector consisting of the PDGF-A-ELP gene in *Escherichia coli* (*E. coli)*, followed by its purification using ITC. Here we chose E. coli for transformation because of its higher efficiency in the introduction of DNA molecules and rapid protein production due to a short generation time of 20 minutes. The purified protein was then characterized using different analytical techniques to help understand the properties of nanoparticles formed at physiological temperatures.

2.2 MATERIAL AND METHODS

2.2.1 Media Preparation

Luria-Bertani (LB) media, Terrific Broth (TB) media, and LB with agar media were prepared for cloning and expression of the protein. 20 grams of LB Broth solution (Life Technologies) were mixed in 1 L of DI water. 47 grams of TB was mixed with 1 L of De-ionized (DI) water and 4 mL of glycerol. 35 grams of LB broth with agar was mixed in 1 L of DI water. The media were autoclaved and allowed to cool.

2.2.2 Cloning and expression of PDGF-ELP

PDGF-ELP was cloned using pET25B^{+} plasmid with 50 pentapeptide repeats of ELP using the protocol described by our lab and others [48, 72]. The sequencing of plasmid, done by GenScript indicated the presence of three restriction enzymes: Mph1103I, NdeI, and

HindIII in the plasmid. The ELP was fused to PDGF-A chain using NdeI and HindIII restriction enzymes and His tag were inserted in the N-terminal using the Mph1103I restriction enzyme. The plasmid consisting of PDGF-A and ELP fused was retransformed in the bacterial host using a heat shock mechanism. *E. coli* (BL21 Star DE3) was obtained from Invitrogen (Lot #: 1932973). In this process, 1 µL of recombinant plasmid was added to 20 µl of thawed *E. coli* in a 1 mL tube and kept on ice for 5 minutes. This was followed by heat shock where the tube was kept in the water bath at 42^{o}C for 2 minutes and then on ice for 2 minutes. This allows competent bacteria to take up the recombinant plasmid. 80 µL of thawed SOC media (Novagen) was added to the tube containing bacterial host and plasmid and the solution was incubated at 37^{o}C for 1 hour. 2 g of carbenicillin was dissolved in 40 mL deionized (DI) H_2O to make a stock solution of 50 mg/mL and aliquoted into 1.5 mL microcentrifuge tubes. A day prior to the bacterial transformation, petri dishes were prepared using 25 mL of agar solution/petri dish including carbenicillin antibiotic (1:1000, 25 µL from stock carbenicillin solution) and stored at 4^{o}C until use. On the day of experiment, , 10 µL of host and plasmid solution was spread on the warm agar plate with antibiotics by the streaking method. The next day, several colonies were observed on the petri dish. A single colony of bacteria was picked up and grown overnight in 50 mL of LB media supplemented with 50 µL of carbenicillin stock solution. After 24 hours, the culture was used to inoculate 1000 mL of TB media with 1000 µL of carbenicillin stock solution. The culture was grown overnight in the incubator shaker located in the BSL 2 facility.

2.2.3 Purification of PDGF-ELP using inverse temperature cycling (ITC)

After 24 hours of incubation, the bacterial culture was centrifuged at 3000 x g at 4^{o}C for 10 minutes. The supernatant was discarded, and the pellet was dissolved in 30 mL PBS with 1:100 ratio of Halt ™ protease inhibitor cocktail (100X) and 0.5 M EDTA solution (100X) (Thermo Scientific). The suspension was sonicated twice on ice for 3 minutes each cycle with 5 seconds ON pulse and 25 seconds OFF pulse and then centrifuged at 15000 x g, 4^{o}C for 30 minutes. The pellet was discarded and 2 mL of 10% w/v of poly(ethyleneimine) (PEI) solution (Sigma Aldrich) was added to the pellet. PEI is positively charged polyelectrolyte and leads to the precipitation of any negatively charged contaminants like DNA from the cell lysate. The solution was centrifuged at 20000 x g, 4^{o}C for 15 minutes. 0.08 grams/1 mL of sodium citrate was added to the supernatant. The solution was incubated at 40^{o}C for 30-40 minutes till it turned cloudy and was then centrifuged (10000 x g) at 40^{o}C for 15 minutes. This is the first hot cycle or spin (H1). The pellet after centrifugation was dissolved in 4 ml of PBS buffer and again centrifuged (15000 x g) at 4^{o}C for 10 minutes. This is the first cold cycle or spin (C1). The supernatant was then used to repeat the hold and cold cycle two more times. 10 µL samples were collected between each spin for SDS PAGE.

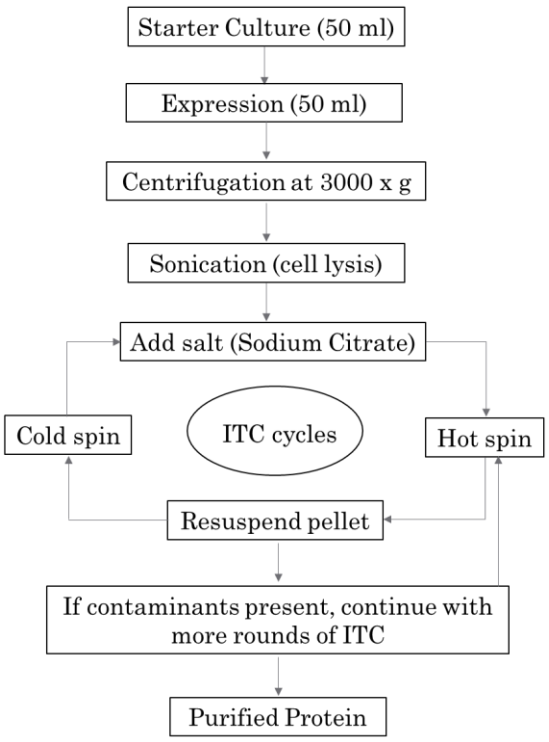

Figure 2.1: Flow chart showing the expression and purification of PDGF-ELP using ITC. Modified from Chilkoti et al. [49]

2.2.4 Physical Characterization

Determination of Protein concentration

Nanodrop spectrophotometer

After three cycles of ITC, the concentration of purified protein was determined by using a NanoDrop spectrophotometer 2000C (Thermo Fisher Scientific). The 2 µL of PBS was used as a blank for the system and then 2 µL of the sample was loaded in the nanodrop and the concentration was measured using the A280 category of protein.

BCA Assay

Diluted albumin from Pierce™ BCA Protein Assay Kit (Thermo Scientific) was used in different concentrations in a 96-well plate as a standard. A set of diluted albumin

standards ranging from 2000 µg/mL to 0 µg/mL (blank) were prepared using the 2 mg/mL albumin ampule provided in the kit. A total volume of the working reagent (WR) was calculated used the formula below:

(no. of standards + no. of unknowns) x (no. of replicates) x volume of WR per sample

For making the WR, 8 parts of BCA reagent A were mixed with 1 part of BCA reagent B. In the 96-well plate, 200 µL of WR and 25 ul of albumin standards were added in triplicate to generate a standard curve. Again, 200 µL of WR and 25 µL of the protein sample to be measured were added in each well in triplicate in the same 96-well plate and incubated in the dark at 37^{o}C for 30 minutes. The plate was allowed to cool for 10 minutes at room temperature. Absorbance was measured at 562 nm using an Infinite M200 Pro plate reader (Tecan). The concentration of the protein was determined by using the standard curve obtained and interpolating the value from it.

SDS PAGE

For SDS-PAGE, a 10 well 4-12% Bis-Tris Gel from Invitrogen (Thermo Fisher Scientific) was used. Loading buffer containing 7.5 µL of LDS sample buffer (Invitrogen) and 3 µL of β-mercaptoethanol (Bio-Rad) for each well was prepared. Each well was loaded with a 30 µL mixture consisting of 19.5 µL samples for all hot and cold spins mixed with 10.5 µL of loading buffer. The supernatant from the third cold spin was diluted to 1 µg/µL for loading. The gel cassette was placed in the SDS-PAGE chamber (Novex). 250 mL of 1X running buffer (made from 20X running buffer by Novex) containing 500 µL of antioxidant (Novex) was poured in the chamber. Both the protein sample mixtures (30

µL) and protein ladder (10 µL, Precision Plus Protein™ Kaleidoscope, Bio-rad) were loaded. SDS PAGE was set to 50 V, 120 mA, 25 W for 5 minutes, followed by 200 V, 120 mA, 25 W for the next 45 minutes. After this, the gel cassette was cooled in running buffer for 10 minutes. Locks on the gel cassette were opened and the gel was allowed to sit in autoclaved water for 5 minutes. The gel stain dye (30 mL, SimplyBlue™ SafeStain, Novex) was used to stain the gel on a rotor for 1 hour. The stain was pipetted out and the gel was washed thrice with autoclaved water to visualize the clear bands of proteins.

Western blot

To perform the western blot, the first step was to run the SDS PAGE gel with 10 µL Ladder, 5 µL PDGF-AA (20 ng), and 10 µL PDGF-ELP (500 ng) in a 10-well gel cassette using the method described above. The gel was removed from the cassette and placed alongside a nitrocellulose membrane in between sponges soaked in 1X transfer buffer containing antioxidant. This setup was placed in the same chamber as described above and was filled with transfer buffer containing antioxidant and methanol (50 mL transfer buffer+ 100 µL antioxidant + 20 mL methanol). Western blot was run for 1 hour at 30 V. The membrane was sealed in a pouch with 10 mL casein to block non-specific binding and kept on the shaker for 30 minutes at 200 rpm. A 1:10000 ratio of primary anti-PDGF antibody (Peprotech) in casein was prepared and filled in a pouch containing the membrane. The pouch was kept on a shaker for 24 hours at 200 rpm, 4^{o}C. Wash buffer containing 0.05% tween was used to wash the membrane thrice. 1:5000 secondary antibody (Rabbit human anti-PDGF AA antibody from Peprotech) was prepared in

casein, sealed in a pouch with the membrane, and kept on a shaker for 1 hour at 200 rpm. After washing thrice with wash buffer, the membrane was stained with Pierce™ 1-Step Ultra TMB blotting solution (Thermo Scientific) for 5 minutes in dark.

Particle size determination

PDGF-ELP was diluted to 7 µM concentration in 1X PBS buffer and used to measure particle size in a Zeta Nano series (Malvern). 1.2 µL of the diluted protein was pipetted in a cuvette and inserted into the Zetasizer at 37^{o}C. Dynamic light scattering was used to determine the diameter of nanoparticles formed at physiological temperatures. Raw data was extrapolated and graphed to demonstrate a single peak representing the diameter of the particle.

Turbidity

To study the formation of nanoparticles at physiological temperature, 100 µl of 15 µM PDGF-ELP was pipetted into 96 well plates in triplicates. The plate with the sample was inserted into an incubator plate reader (Infinity M200 Pro, Tecan) and turbidity was determined spectrophotometrically by measuring the absorbance at 350 nm starting from 25^{o}C till 40^{o}C with a gradient of 2^{o}C. Absorbance vs temperature was graphed to determine the transition temperature of the nanoparticle.

2.3 RESULTS

2.3.2 Cloning and expression of PDGF-ELP

The plasmid consisting of 50 pentapeptide repeats of ELP and a single chain of PDGF A is shown below:

Sequence for Mph1103I-6xHIS-PDGF-A-3 x GAL linker NdeI
(378bp 126 aa from XM_011515419.3)
atgCATCACCATCACCATCAC

agcatcgaggaagctgtccccgctgtctgcaagaccaggacggtcatttacgagattcctcggagtcaggtcgaccccacgtc
cgccaacttcctgatctggcccccgtgcgtggaggtgaaacgctgcaccggctgctgcaacacgagcagtgtcaagtgccagc
cctcccgcgtccaccaccgcagcgtcaaggtggccaaggtggaatacgtcaggaagaagccaaaattaaaagaagtccagg
tgaggttagaggagcatttggagtgcgcctgcgcgaccacaagcctgaatccggattatcgggaagaggacacgggaaggc
ctagggagtcaggtaaaaaacggaaaagaaaaaggttaaaacccacc
GGCGCCcttggtgcgctgggcgcactt
CATATG

ELP Motifs V40C2 Mph1103I-NdeI-ELP-HindIII
atgCATCACCATCACCATCACGGTGGTGAAAATCTGTATTTTCAGGGCGGCGGTgGGCCGGGCG
TGGGTCATATG
GGGCCGGGCGTGGGT GTTCCGGGCGTAGGT GTCCCAGGTGTGGGC GTACCGGGCGTTGGT
GlyProGlyValGly **ValProGlyValGly**

GTTCCTGGTGTCGGC GTGCCGGGCGTGGGT GTTCCGGGCGTAGGT GTCCCAGGTGTGGGC
GTACCGGGCGTTGGT GTTCCTGGTGTCGGC GTGCCGGGCGTGGGT GTTCCGGGCGTAGGT
GTCCCAGGTGTGGGC GTACCGGGCGTTGGT GTTCCTGGTGTCGGC GTGCCGGGCGTGGGT
GTTCCGGGCGTAGGT GTCCCAGGTGTGGGC GTACCGGGCGTTGGT GTTCCTGGTGTCGGC
GTGCCGGGCGTGGGT GTTCCGGGCGTAGGT GTCCCAGGTGTGGGC GTACCGGGCGTTGGT
GTTCCTGGTGTCGGC GTGCCGGGCGTGGGT GTTCCGGGCGTAGGT GTCCCAGGTGTGGGC
GTACCGGGCGTTGGT GTTCCTGGTGTCGGC GTGCCGGGCGTGGGT GTTCCGGGCGTAGGT
GTCCCAGGTGTGGGC GTACCGGGCGTTGGT GTTCCTGGTGTCGGC GTGCCGGGCGTGGGT
GTTCCGGGCGTAGGT GTCCCAGGTGTGGGC GTACCGGGCGTTGGT GTTCCTGGTGTCGGC
GTGCCGGGCGTGGGT GTTCCGGGCGTAGGT GTCCCAGGTGTGGGC GTACCGGGCTGCGGT
GTTCCTGGTGTCGGC GTGCCGGGCGTGGGT GTTCCGGGCGTAGGT GTCCCAGGTGTGGGC
GTACCGGGCTGCGGT GTTCCTGGTGTCGGC GTGCCGGGCTGGCCG
TGA TAA TTCGAGCTCCGTCGAC Aagctt

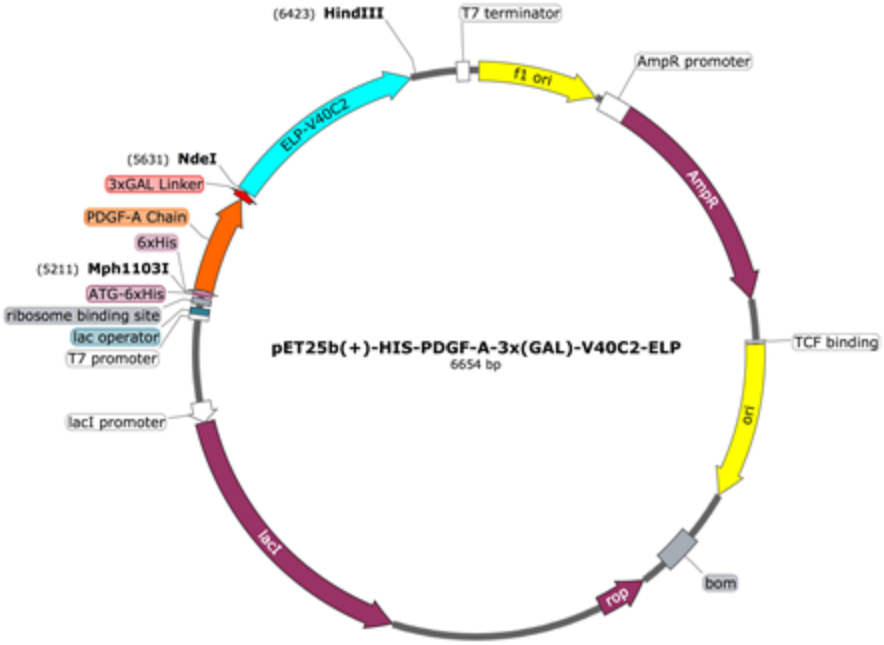

Figure 2.2: Plasmid consisting of recombinant fusion protein PDGF-A-ELP

2.3.3 Physical Characterization

Determination of Protein Concentration

Protein concentration was found to be between 2 and 3 mg/mL using both the Nanodrop and BCA.

SDS PAGE

With each cycle of ITC, the number of bands in the gel reduces, eventually leaving a single purified band obtained after 3 cycles of bacterial lysate purification. The band corresponds to ~37 kDa which matches the theoretical molecular weight of our fusion protein PDGF-ELP.

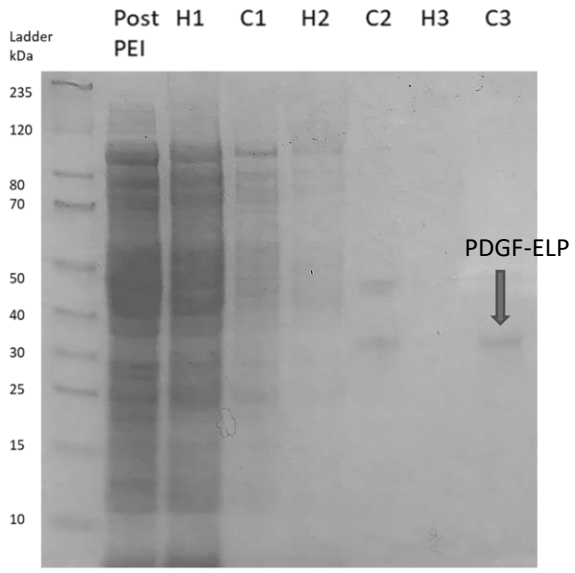

Figure 2.3: SDS PAGE gel: Lane 1 is the molecular weight ladder; Lane 2 is the protein in the bacterial lysate before purification; Lane 3 is the contaminants after H1 spin. Several bands indicate non-purified protein; Lane 4 represents protein after C1 spin. Fainter bands show the removal of contaminants; Lane 5 represents contaminants after H2 spin. The second hot spin has lesser bands as compared to the first hot spin. Lane 6 represents protein after C2 which shows only a few bands after purification. Lane 7 represents supernatant which does not show any bands because contaminants have been removed after 3 cycles of ITC purification. Lane 8 is the final purified protein after third cold spin C3 representing a single band at ~37 kDa which is PDGF-A-ELP.

Western Blot

The protein transferred to the nitrocellulose membrane was subjected to the monoclonal anti-PDGF antibody. The figure below shows that the fusion protein was reactive to the anti-PDGF antibody showing a single band at ~37 kDa.

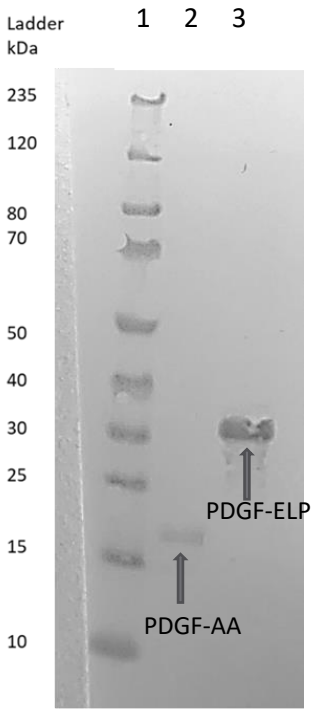

Figure 2.4: Western blot: Lane 1: Molecular Weight Ladder; Lane 2: PDGF-AA used as Control ; Lane 3: PDGF-ELP

Particle size determination

Particle size of 624 nm was obtained from the Zetasizer. A single sharp peak at ~620 nm is observed in the chromatogram which represents the diameter of the nanoparticles formed at 37^{o}C. The polydispersity index (PDI) was obtained as 0.039 under these conditions. For nanoparticles, PDI is representative of how monodisperse/polydisperse the sample is. Values less than 0.1 means that the sample is monodisperse i.e. there is high uniformity of particle sizes [77]. Hence, we can say that our solution is monodisperse at 37 ^{o}C, 7 µM concentration.

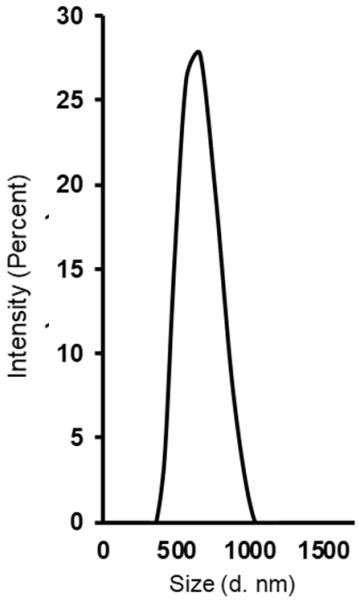

Figure 2.5: Chromatogram of PDGF-ELP nanoparticles (~620 nm) run on a Zetasizer. The size obtained from the graph is ~620 nm.

Turbidity

As seen from the graph below, the transition temperature of the nanoparticles is around 37°C which is the physiological temperature of the human body. The absorbance plateaus from 25°C to 35°C and then starts increasing close to 37 °C. This indicates that the formation of nanoparticles has begun and keeps increasing as the temperature rises to 42°C.

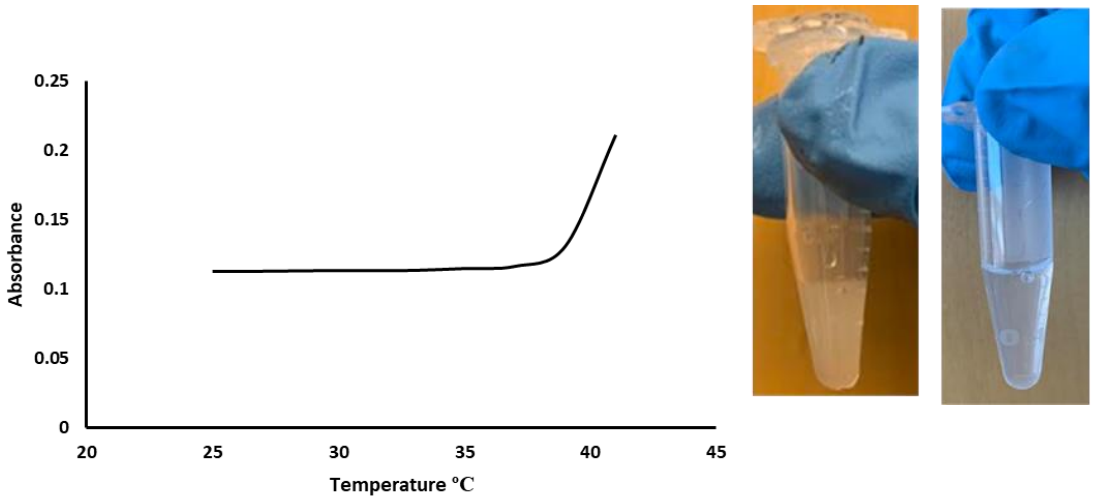

(A) (B)

Figure 2.6: Determination of phase transition temperature and turbidity**.** a) The turbidity graph shows the increase in absorbance around 37°C which peaks as the temperature increases to 42°C. b) The first tube shows the cloudy PDGF-ELP solution at 40°C resulting due to nanoparticle formation, the second tube shows a clear PDGF-ELP solution in the soluble form at 4°C.

2.4 SUMMARY

The development of fusion protein using an *E.coli* host led to the formation of PDGF-ELP of length 398 amino acid, molecular weight 37.229 kDa, and charge at pH 7.4 as 4.38. The positively charged protein allowed for purification using ITC and PEI. Physical characterization using SDS-PAGE revealed the presence of a single band after a third hot spin, by getting rid of impurities at each ITC step. The presence of PDGF-A in the fusion protein was further confirmed by western blot with an anti-PDGF-A antibody. Nanodrop and BCA assays were used to determine the concentration of the protein obtained after the third hot spin, which ranged between 2-3 mg/ml. The size of the nanoparticle formed at 37^{o}C was ~620 nm. Using the turbidity experiment, the formation of nanoparticles can be seen both physically with a more cloudy/turbid solution at 40^{o}C as compared to 4^{o}C and experimentally by measuring the absorbance of the fusion protein with an increase in temperature. In the graph, nanoparticles start forming around 37^{o}C and keep the increase as the temperature rises to 42^{o}C.

CHAPTER 3: CELL PROLIFERATION ASSAY

3.1 INTRODUCTION

PDGF activates cell surface receptors α and β present on fibroblasts in chronic wounds. Peus et al. demonstrated the increased level of messenger mRNA for both the receptor types on fibroblasts [56]. Immunostaining for the receptors in the granulation tissue layer from wounds showed the localization of the receptors on these mesenchymal cells [57]. Yu et al. proposed that both PDGF AA and PDGF BB promote the migration of murine fibroblasts [58]. Proliferation ability of endothelial cells in the presence of PDGF is still debatable. Endothelial cells express only β receptors [59]. A study conducted by Zetter et al. suggested that PDGF plays a role in human umbilical vein endothelial cell (HUVEC) growth [60]. Hence, we tested the proliferation ability of both fibroblasts and HUVEC in the presence of our fusion growth factor as well as low serum media.

3.2 MATERIAL AND METHODS

Dulbecco's Modified Eagle's Medium (DMEM by Gibco) supplemented with 10% v/v FBS (Fetal Bovine Serum by Gibco) and 1% v/v Pen/Strep were used to grow and maintain fibroblasts (human primary cell line from Lifeline Cell Technologies) in a sterile incubator (21% O2, 5% CO2 at 37 ^{o}C) and was called complete DMEM. Cells were cultured in 125 cm^2 tissue culture flasks and were used between passages 2 and 6 for the proliferation experiment. Fibroblasts were seeded in a 96 well plate (Falcon) at density 2 X 10^3 cells/well in 200 µL/well complete DMEM and grown for 24 hours in the incubator (Day

1). After overnight growth, the cells were washed with PBS buffer, and grown in serum-free media, meaning that the old media was aspirated and replaced with DMEM + 1% v/v Pen/Strep without supplement (Day 2). Four conditions were used in the experiment: i) Control- cells were grown in serum-free media, ii) cells grown in serum-free media+ 5 nM PDGF, iii) cells were grown in serum-free media+ 5 nM PDGF-ELP and iv) cells were grown in serum-free media+ 5 nM ELP. A control positive condition (cells were grown in complete DMEM) was also used in each plate, not for experimental purposes, but to check the working of the cell system in general. 48 hours after adding the conditions (Day 4), the wells were washed and replaced with 100 µl/well serum-free media and 20 µl/well CellTiter 96® AQ_{ueous} (by Promega). This is a non-radioactive, colorimetric method used to measure the number of viable cells in a proliferation assay. After 2 hours of incubation at 37 ^{o}C, the absorbance was measured at 492 nm using Infinite M200 Pro plate reader by Tecan. A cell number in each well and the fold change were calculated using the standard curve generated parallelly. Experiments were repeated in triplicates.

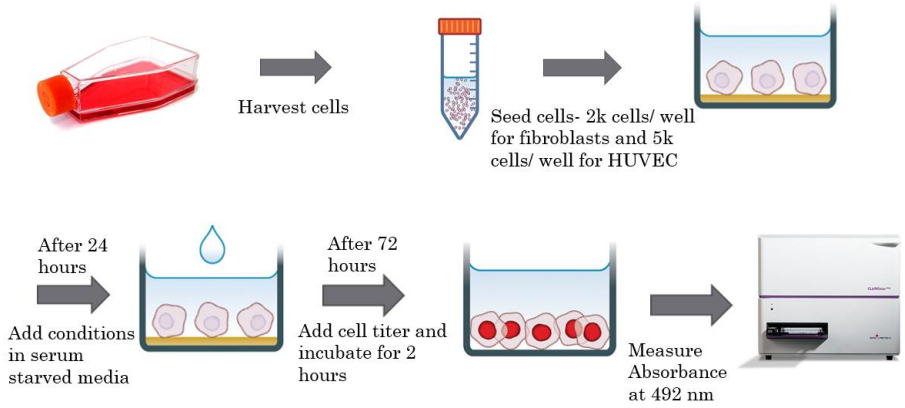

Figure 3.1: Cell proliferation protocol using CellTiter to estimate cell number and fold change. Some individual images in the flow diagram is modified from [80]

The proliferation assay was conducted in a similar manner using HUVEC from Life Technologies. HUVEC cells were maintained in Medium 200 media + low serum growth supplement (Life Technologies) + 1% v/v Pen/Strep (complete M200 media). Cells were grown in 75 cm^2 tissue culture flasks and the only cells between passage number P2-P6 were used. Cells were seeded in a 96 well plate at density 5 X 10^3 cells/well in 200 µl/well on day 1. On day 2, the media was replaced with M200 + 2% v/v FBS and 1% v/v Pen/Strep (serum-free M200). Four conditions were used in the experiment: i) Control- cells were grown in serum-free media, ii) cells grown in serum-free M200+ 5 nM PDGF, iii) cells were grown in serum-free M200+ 5 nM PDGF-ELP and iv) cells were grown in serum-free M200+ 5 nM ELP. A control positive condition (complete M200) was also used in each plate, not for experimental purposes, but to check the working of the cell system in general. On Day 4, cells were measured using CellTiter using the same protocol as fibroblast cells.

3.3 DATA ANALYSIS

Data shown are mean ± standard error of the mean (SEM). N value of 5 or more replicates was used. One-Way ANOVA followed by posthoc Tukey HSD test was used for statistical analysis of the data. Pvalue of <0.05 is considered statistically significant.

3.4 RESULTS

PDGF-ELP fusion protein cultured in serum-starved DMEM shows a statistically higher cell number and thus higher fold increase as compared to the control, PDGF, and ELP groups. PDGF-ELP showed a ~1.8-fold increase in fibroblast proliferation and a ~3.5-fold increase in HUVEC proliferation suggesting enhanced cell growth and biological activity of the fusion protein. PDGF and ELP itself had no/minimal effect on fibroblast proliferation.

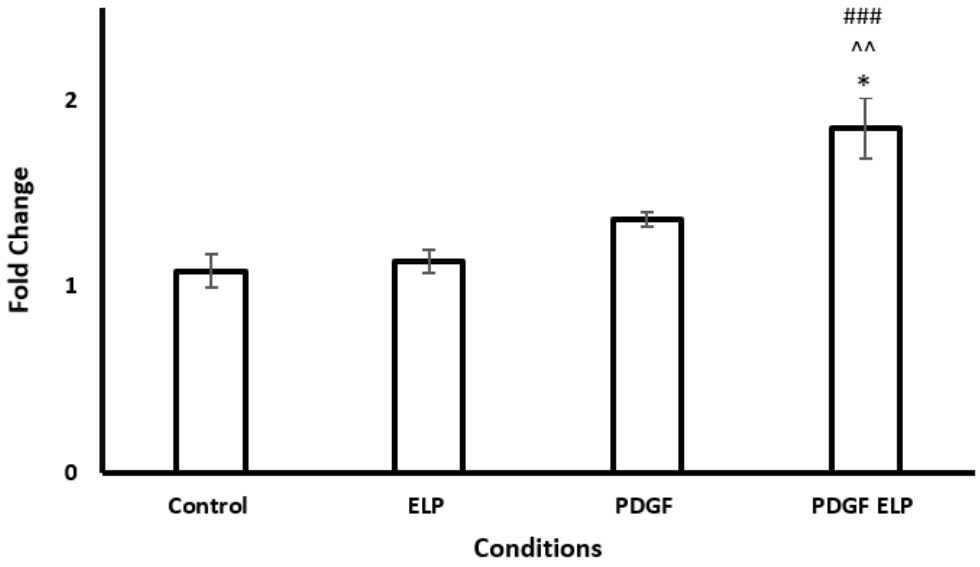

Figure 3.2: Effect of PDGF-ELP on fibroblast proliferation. Cell proliferation as a function of cell growth was studied under serum-starved using different conditions. The cell number was measured using CellTiter post 48-hour of treatment with ELP, PDGF, PDGF-

ELP (5 nM in each group), and compared with Control (only media). Data are presented as mean ± SEM (n = 6). * indicates a comparison between PDGF and PDGF-ELP (*p<0.05). ^ indicates comparison between ELP and PDGF-ELP (^^p<0.01) while # indicates comparison between Control and PDGF-ELP group (###p<0.001).

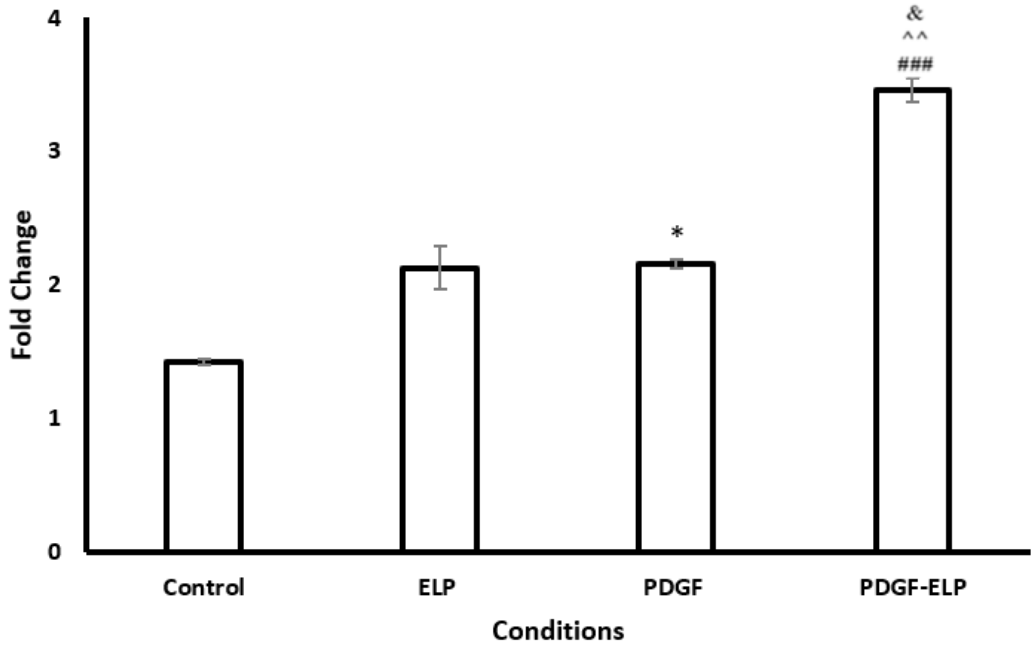

Figure 3.3: Effect of PDGF-ELP on HUVEC proliferation. Cell proliferation as a function of cell growth was studied under serum-starved using different conditions. The cell number was measured using CellTiter post 48-hour of treatment with ELP, PDGF, PDGF-ELP (5 nM in each group), and compared with Control (only media). Data are presented as mean ± SEM (n = 3). * indicates a comparison between PDGF and Control (*p<0.05). ^ indicates comparison between ELP and PDGF-ELP (^^p<0.01), # indicates comparison

between Control and PDGF-ELP group (###p<0.001) while & indicates comparison between PDGF and PDGF-ELP (&p<0.05)

3.5 SUMMARY

The goal of this section was to investigate and compare the proliferative ability of PDGF-ELP with PDGF and ELP. Both fibroblasts and HUVEC showed increased fold change when PDGF-ELP in 5 nM concentration was used. For fibroblast and HUVEC, ~1.8 fold change and ~3.4 fold change were observed respectively. This result was statistically higher than PDGF and ELP at 5 nM concentrations suggesting higher biological activity at this concentration for the fusion protein.

CHAPTER 4: MIGRATION ASSAY USING FIBROBLASTS

4.1 INTRODUCTION

Cell migration plays an important role in many biological processes like tissue repair, organogenesis, angiogenesis, and tumor growth. Several studies have shown that PDGF can induce proliferation, migration, and differentiation [61]. PDGF exerts such functions by binding to its receptors, dimerizing, and activating a cascade of catalytical activity. This is followed by its autophosphorylation on tyrosines with specificity, which act as anchoring sites for signaling molecules that are within the cells. The association of SH2 containing adapter proteins activates mitogen-activated protein kinase (MAPK) thereby enhancing cell proliferation signals [62].

Earlier studies have demonstrated the chemoattractant properties of PDGF using a Boyden's chamber [63]. Recent studies have used fabricated scaffold for release of PDGF that gives rise to migration of skin fibroblasts in a controlled manner [64]. Hence, in this chapter, we have performed a monolayer scratch assay to study the fibroblast cell migration by measuring the wound closure time on a confluent cell layer. The scratch assay is a simple, cost-effective, and well-established measure of cell migration *in vitro* [65]. In our project, a scratch assay is particularly suitable because it mimics cell migration *in vivo* and allows imaging live cells during different time periods.

4.2 MATERIAL AND METHODS

Human dermal fibroblasts were maintained in Dulbecco's modified Eagle's medium (DMEM)+ 10% v/v FBS+ 1% Pen/Strep (complete DMEM). Cells between passages 2-6

were used for the experiment. Cells were harvested and seeded in 24 well plates (Falcon) at a density of 5 X 10^4 cells/well in 500 µL complete DMEM (day 1). After 48 hours of seeding (day 3), the cells were serum-starved, i.e. the complete DMEM was aspirated out of the well and replaced with DMEM+1% v/v Pen/Strep (serum-free DMEM), without supplement for 24 hours. On day 4, the cell monolayer was scared in the well using 200 µL pipette tips. To remove debris and dead cells, the wells were washed with PBS buffer and replaced with 500 µL of serum-free media. Four conditions were used in the experiment: i) Control- cells were grown in serum-free media, ii) cells were grown in serum-starved free+ 5 nM PDGF, iii) cells were grown in serum-free media+ 5 nM PDGF-ELP and iv) cells were grown in serum-free media+ 5 nM ELP. A control positive condition (cells were grown in complete DMEM) was also used in each plate, not for experimental purposes, but to check the working of the cell system in general. To obtain the same field during image capturing, a reference line was made at the bottom of the plate with a tip marker.

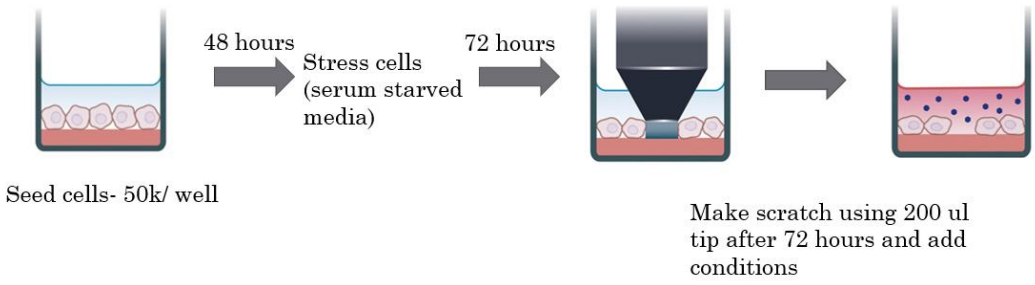

Figure 4.1: Migration assay protocol. Scratching the cell monolayer with a pipette tip, adding conditions and imaging at 0, 24, and 48 hours. Some individual images in the flow chart is modified from [81]

Scratch closure was studied by using a phase-contrast microscope at 10X for image acquisition. At time points 0-hour, 24 hours, and 48 hours after scratching the monolayer of cells, the image was captured by matching the reference point and keeping the reference line outside the capture image field using the Olympus CKX31 camera and Magnifier Software. During the period from 0 to 48 hours, cells were incubated in the tissue culture incubator (21% O_2, 5% CO_2 at 37 ^{o}C). The images obtained were analyzed quantitatively using the NIH ImageJ software. The area for wound closure was measured using the software at different time points. For further analysis, the number of cells in the scratch were measured and plotted in a graph. The % wound closure was calculated using the formula below:

$$\%\, wound\ closure = 100 - [\left(\frac{A(n)}{A(0)}\right) * 100]$$

Where A(n) is the area of the wound at day n (n=0, 1, and 2) and A(0) is the area of the wound at day 0.

4.3 DATA ANALYSIS

Data shown are mean ± standard error of the mean (SEM). N value of 6 or more replicates was used. One-Way ANOVA followed by posthoc Tukey HSD test was used for statistical analysis of the data. P-value of <0.05 is considered statistically significant.

4.4 RESULTS

To evaluate whether our four different conditions had any effect on the migration of fibroblasts grown in serum-free DMEM, a series of scratch assays were carried out and the experiments were repeated thrice. A scratch of uniform width was created in each well. The purpose of serum-starving the cells 48 hours after seeding, was to control the cell growth and migration for obtaining enough time points to capture the image. Images were captured immediately (0-hour time point), after 24 hours of incubation (24-hour time point) and after 48 hours of incubation (48-hour time point). % Wound closure was calculated using the formula stated above.

At the end of 24 and 48-hour incubations, the PDGF-ELP group showed enhanced migration of cells towards the scratch and thus, significantly increased wound closure by PDGF-ELP as compared to the control. PDGF treated groups also showed significant wound closure as compared to the control at 24 and 48-hour time point. The mean % wound closure after 48-hour time point for the PDGF-ELP treated group and PDGF treated group was 88.13% and 79.18% respectively, whereas Control and ELP treated groups had 59.9% and 69.2% wound closure, respectively. The number of cells migrating in the wound area is also graphed below.

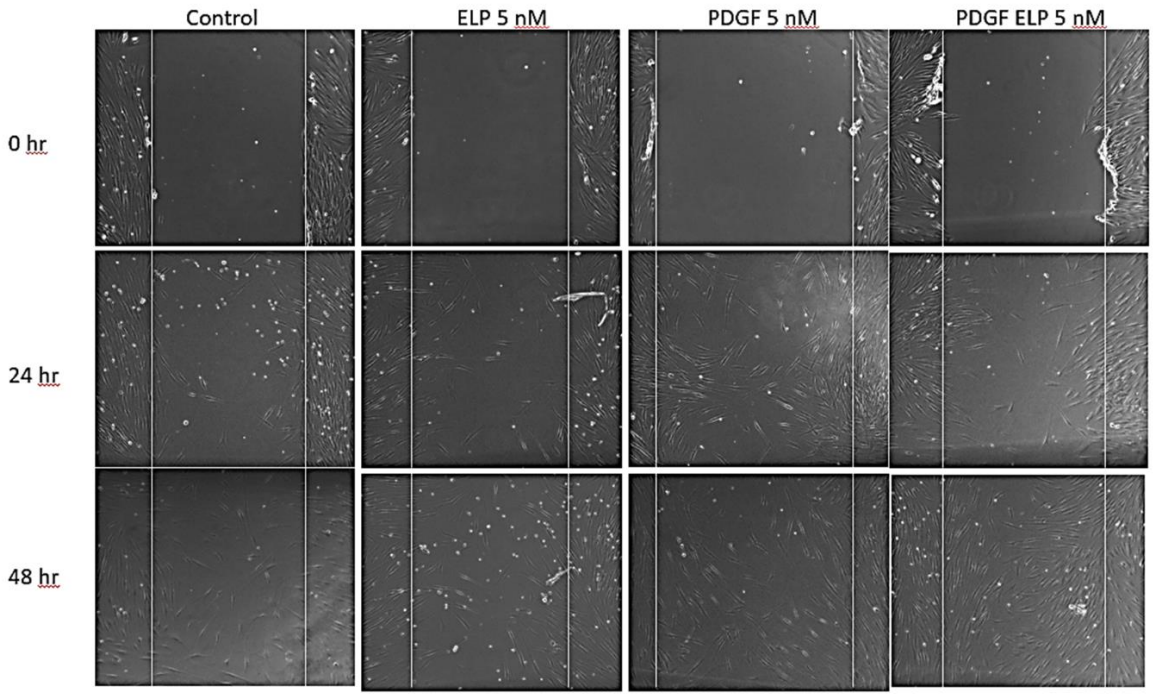

Figure 4.2: Effect of PDGF-ELP on fibroblast migration. Representative phase-contrast microscope images of fibroblasts with different conditions at 0, 24, and 48 hour time points after scratch initiation.

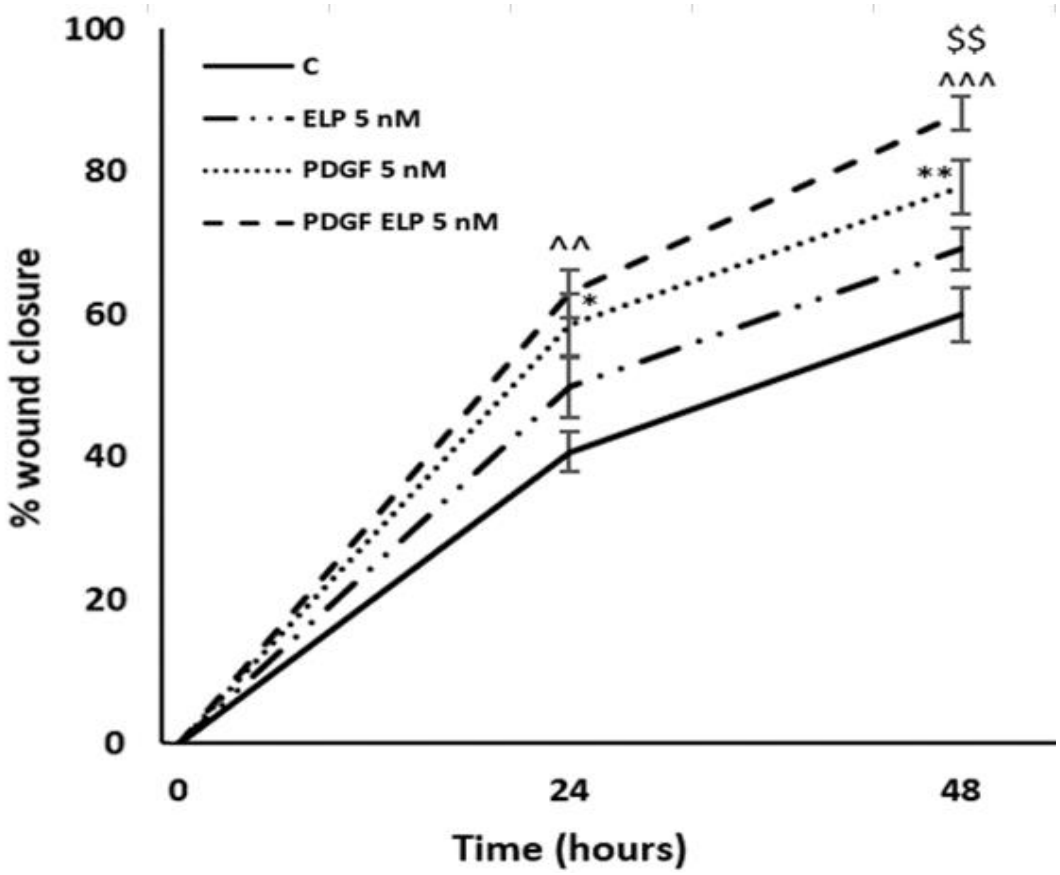

Figure 4.3: Graphical representation of the effect of PDGF-ELP on fibroblast migration. The effect of ELP, PDGFand PDGF-ELP (5 nM) on % wound closure at 0, 24, and 48 h time points were studied and presented as plotted. ^ represents a comparison between PDGF-ELP and Control. ^^ means $p<0.01$ between PDGF-ELP and Control at 24 h time point. ^^^ means $p<0.001$ between PDGF-ELP and Control at 48 h time point. * represents a comparison between PDGF and Control. * means $p<0.05$ between PDGF and Control at 24 h time point. ** means $p<0.01$ between PDGF and Control at 48 h time point. $^{\$}$ represents the comparison between PDGF-ELP and ELP ($^{\$\$}p<0.01$)

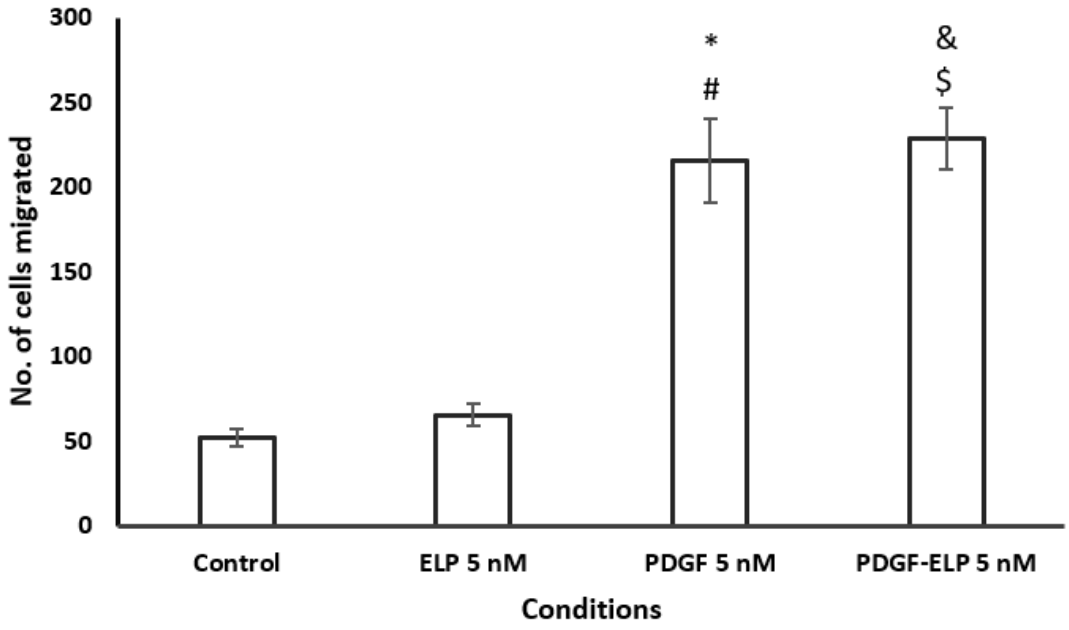

Figure 4.4: Number of cells migrated in the scratch area. Cell monolayer was conditioned with ELP, PDGF, and PDGF-ELP at 5 nM concentration. * represents a comparison between PDGF and Control (*$p<0.0001$) and # represents a comparison between PDGF and ELP ($^{\#}p<0.0001$). & represents comparison between PDGF-ELP and Control ($^{\&}p<0.0001$) and $ represents comparison between PDGF-ELP and ELP ($^{\$}p<0.0001$)

4.5 SUMMARY

In this section, the ability of fibroblasts to migrate and close the scratch formed on the monolayer was assessed using different conditions at different time points. The results are shown in three ways as shown by the images and graphs plotted above. Just by looking at the images, one can say that more number of cells migrated in the scratch with PDGF and PDGF-ELP at 5 nM concentrations. For graphical analysis, PDGF and PDGF-ELP show statistically higher % wound closure as compared to ELP and Control at 24 hr and 48 hr time points which can be seen as the dashed lines on the graph. Because fibroblast migration is difficult to demarcate due to the shape of the cells, we used another analysis method to measure the migrative ability of fibroblasts. The number of cells within the scratch area were counted for each condition and time point and represented in a bar graph. The number of cells migrated into the scratch were statistically higher with PDGF and PDGF-ELP conditions at 5 nM concentration. Hence, from this chapter, we evaluated and analyzed the migration of fibroblasts, and both the nanoparticles and the native protein showed similar activity *in vitro*.

CHAPTER 5: ENDOTHELIAL CELL TUBE FORMATION ASSAY

5.1 INTRODUCTION

Angiogenesis is vital for embryonic development, organ formation, and growth, and wound healing [69]. The newly formed blood vessel support oxygen supply and nutrient replenishment to the tissue and removal of debris. During wound healing, angiogenesis is initiated immediately during the first stage of the process. Capillary endothelial cells have shown to have receptors for PDGF suggesting that PDGF may have a direct role in angiogenesis [29, 67]. PDGF receptor is specific for cord/tube forming endothelial cells contributing to angiogenesis *in vitro* [31]. An *in vivo* experiment using the chick chorioallantoic membrane revealed enhanced vessel formation in the presence of PDGF. While both PDGF-AA and BB affected angiogenesis, PDGF-BB was a more potent chemotactic agent than PDGF-AA [66]. Research on the application of PDGF-BB gel to study the wound healing effects on diabetic mice was conducted which showed that a dose-dependent PDGF-BB treatment enhanced angiogenesis studied using immunohistological methods [68]. However, the angiogenic effect of PDGF on tube formation is not as strong as other growth factors like basic FGF and VEGF.

The tube formation/angiogenic assay is a fast and quantitative method for stimulating the cord/tube formation capability in response to signals that cause blood vessel formation. Endothelial cells are seeded on a basement membrane matrix which then differentiates and forms capillary-like structures that can be visualized using a phase-contrast microscope or fluorescence/confocal microscope after staining with calcein

dye. Depending upon the stimuli, tube formation begins within 2-6 hours in this assay [70]. The number of tubes, nodes, and meshes can be quantitively calculated from the images obtained. In this experiment, we used primary endothelial cells such as HUVEC.

5.2 MATERIALS AND METHODS

Human primary HUVEC (passages between p2-p6, Life Technologies) cells were cultured in a 75 cm^2 tissue culture flask in M200 phenol red-free media with low serum growth supplement (Life Technologies) until it was at least 80% confluent. Matrigel (Corning Life Sciences) was thawed on ice overnight at 4 ^oC (day 1). On day 2, 250 µl/well (10 mg/ml) of Matrigel was spread evenly over the 24-well plate (Falcon). The plate with Matrigel was incubated for 30-40 minutes at 37^oC to allow to Matrigel to gel. HUVEC cultured in tissue culture flask was trypsinized, harvested, and concentrated in non-supplemented Medium 200 PRF. 1.2 X 10^5 cells in 300 µL from the cell suspension were pipetted onto the Matrigel.

Three conditions were used in the experiment: i) control- cells grown in 2% free media, ii) cells grown in 2% FBS media+ 5 nM PDGF, iii) cells grown in 2% FBS media+ 5 nM PDGF-ELP. A control positive condition (cells were grown in complete DMEM) was also used in each plate, not for experimental purposes, but to check the working of the cell system in general. The three conditions were added in separate wells in triplicates. After 16-18 hours of incubation at 37^oC (day 3), the wells were washed twice with 2X Hank's Balanced Salt Solution (HBSS). To prepare calcein dye for cell and tube staining, 8 µg/ml of calcein-AM was prepared, 200 µl of the dye was pipetted into each well, and

incubated at 37 ^{o}C for 30 minutes. The wells were washed twice with 2X HBSS. A fluorescence microscope (Olympus IX81®) was used to capture images of each well. The number of tubes, nodes, and meshes were counted NIH ImageJ software and graphed as shown in the next section.

5.3 DATA ANALYSIS

Data shown are mean ± standard error of the mean (SEM). N value of 3 replicates was used. One-Way ANOVA followed by posthoc Tukey HSD test was used for statistical analysis of the data. P-value of <0.05 is considered statistically significant

5.4 RESULTS

The ability of PDGF-ELP to form capillary-like tubes, meshes, and nodes represented by green dots is studied using an angiogenesis tube assay using HUVEC cells. A concentration of 5 nM for PDGF and PDGF-ELP was used for the experiment. After an 18 hour incubation period, images were captured using a confocal microscope. Both PDGF and PDGF-ELP had a significantly higher number of tubes, nodes, and meshes formed than the vehicle control group which was the serum-free media without the presence of growth factors. There was not a significant difference between PDGF and PDGF ELP at 5 nM concentrations.

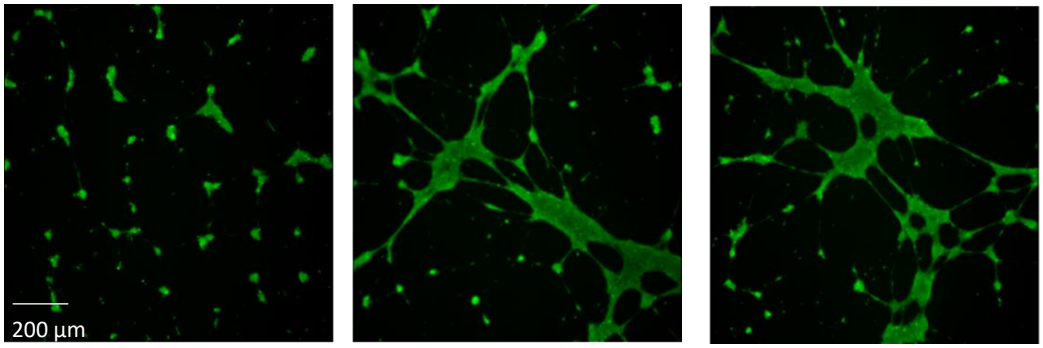

A: Control B: PDGF A C: PDGF-ELP

Figure 5.1: Effect of PDGF-ELP on tube formation and angiogenesis. Fluorescent images of endothelial cells forming capillary-like structures on Matrigel (N=3). Three different conditions are (A) Growth factor free media, (B) PDGF-A (5 nM) with media, and (C) PDGF-ELP (5 nM) with media. Image (A) shows only nodes represented by green dots without the formation of meshes and tubes. Image (B) and (C) shows nodes, as well as capillary like dtructures joining two nodes. Meshes are formed when three or more nodes form a network through tubes. Scale bar = 200 µm

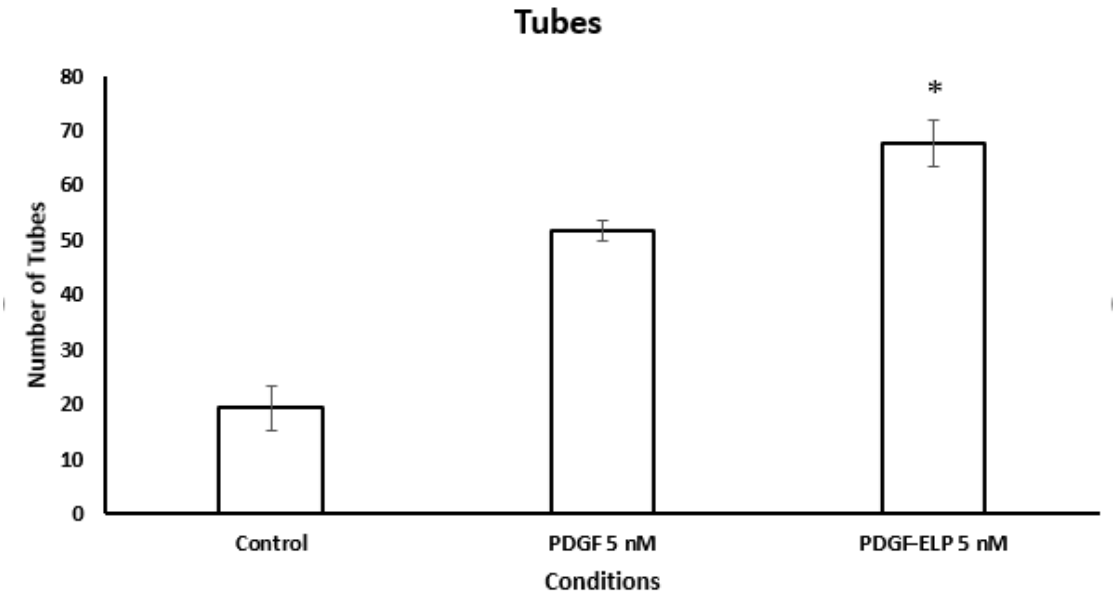

(A) Number of tubes

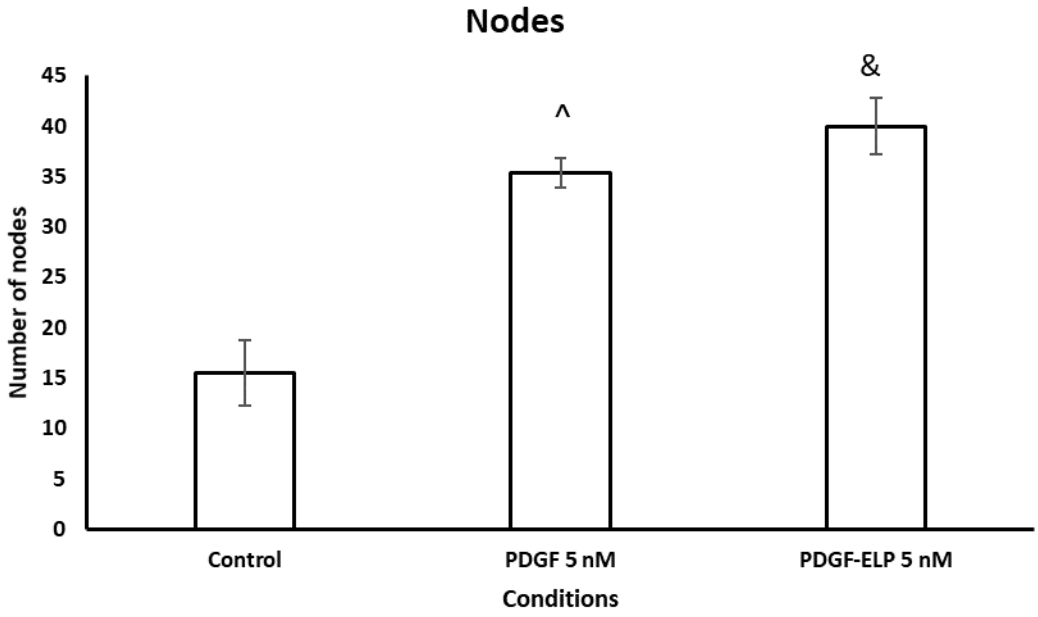

(B) Number of nodes

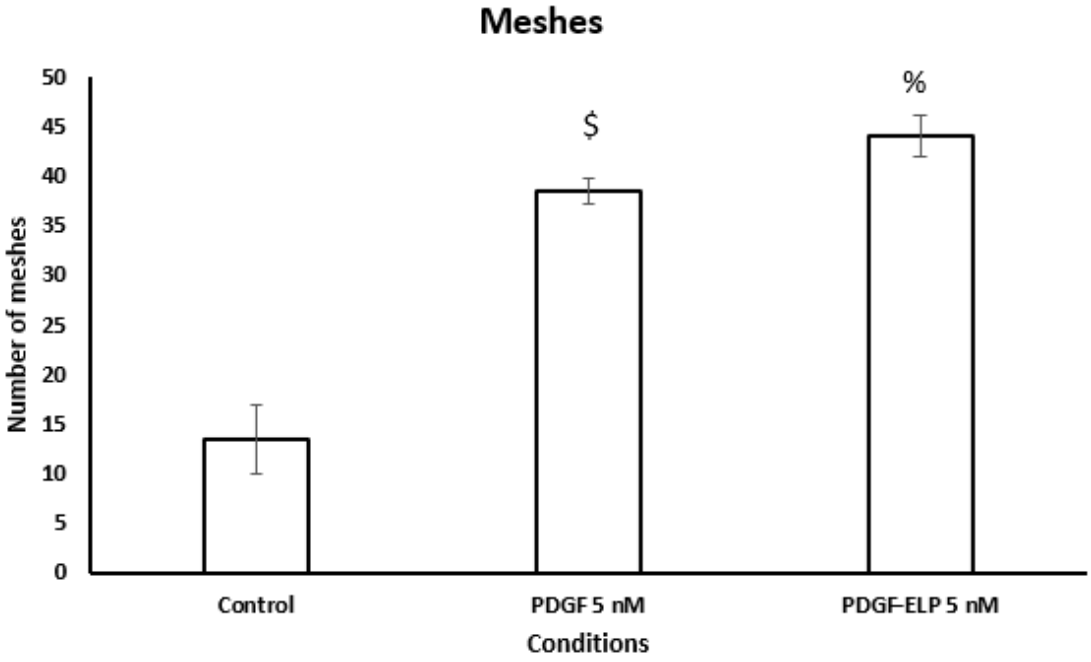

(C) Number of meshes

Figure 5.2: Graphical representation of the number (A) tubes, (B) nodes, (C) meshes formed in endothelial tube assay (N=3). **(A)** Number of tubes formed in different conditions. * represents a comparison between PDGF-ELP and Control (*$p<0.0001$). **(B)** Number of nodes formed in different conditions. ^ represents a comparison between PDGF and Control (^$p<0.0001$) and & represents a comparison between PDGF-ELP and Control. **(C)** Number of meshes formed in different conditions. $ represents a comparison between PDGF and Control ($^{\$}p<0.0001$) and % means comparison between PDGF-ELP and Control ($^{\%}p<0.0001$)

5.5 SUMMARY

The ability of HUVEC cells to form multicellular structures in the presence of PDGF and PDGF-ELP at 5nM concentration was evaluated in this section. HUVEC seeded on Matrigel-coated wells were imaged using fluorescent microscopy after 18 hours by staining with calcein dye. The green structures visible on the black background helped us distinguish the network forming ability of the cells under different conditions. The number of tubes, nodes, and meshes formed were counted using ImageJ software. PDGF-ELP formed statistically higher number of tubes than control at 5 nM concentration. Both PDGF and PDGF-ELP showed a higher number of meshes and nodes at the same concentration. From this experiment, we can conclude that both the fusion protein and the native PDGF have similar angiogenic properties. Furthermore, this can have a positive impact on wound healing as their activity was better as compared to the control with HUVEC cells seeded in low growth factor media.

CHAPTER 6: DISCUSSION AND CONCLUSION

Chronic wounds are an economic burden to the patients, caretakers, and health care industry. The annual wound care market in the medical system is expected to rise to $15-$20 billion by 2024 [71]. Chronic wounds get arrested in the prolonged inflammatory stage of healing due to underlying factors of hypoxia, stress, age, and underlying health conditions amongst other factors (2). While there are several treatment options as summarized in Table 1. There are limitations associated with each method which includes the high cost of treatment and the requirement of a skilled professional. Moreover, these treatments do not always show satisfactory outcomes. Advances in the study of the pathophysiology of chronic wound environment have led to the use of therapies like growth factors for treatment. Becaplermin, the only available FDA approved topical gel treatment for diabetic ulcers, shows mixed efficacy results in randomized trials and there isn't enough prolonged study data to support its use especially one that weighs the risk to benefit ratio. Hence, considering the positive effects of exogenously applied growth factors, we used ELP tagged growth factor PDGF-A for testing the wound healing properties in the *in vitro* system.

In this study, PDGF-ELP has generated as nanoparticles with particle size ~600 nm as shown using a Zetasizer. PDGF-ELP was purified using ITC. ELP can undergo a phase transition and thus a protein fused with ELP also shows the same characteristics as native ELP. The ability of PDGF-ELP to form nanoparticles above the transition temperature and remain soluble in the solution below the transition temperature allows

for the removal of soluble and insoluble contaminants, respectively, using consecutive rounds of hot and cold spins as described above. This non-chromatographic method is a much cheaper alternative for protein purification. ELP 50 pentapeptide repeats were fused at the C terminus of PDGF-A. The phase transition temperature of the fusion protein was found to be ~37^{o}C using a turbidity measuring experiment thus warranting the presence of nanoparticle fusion growth factor in the wound at physiological temperatures.

Our goal was to design a novel growth factor drug depot system that elicits the individual properties of both PDGF-A and ELP. Cellular biological activity of the growth factor at 5 nM concentration was studied using proliferation, migration, and tube assays. Fibroblast and endothelial cell proliferation assays showed significantly higher cell fold change for PDGF-ELP when compared to ELP, PDGF A, and vehicle control. In the presence of PDGF-ELP, fibroblasts expressed a ~2 fold increase and HUVEC expressed a ~3.5 fold increase. PDGF-ELP showed a ~90% wound closure at 48 hours after scratch initiation as compared to ~60% wound closure in-vehicle control-treated wells. Further, enhanced angiogenesis using PDGF-ELP as shown in the endothelial tube assay also supports our hypothesis that our fusion protein improves wound healing in *in vitro* systems.

PDGF-ELP outperforms PDGF which is supported by significantly higher fibroblasts and HUVEC proliferation data. Native PDGF shows statistically higher % wound closure in migration assay as compared to the control. However, in the proliferation assay, the native protein did not have significantly higher number of cells in fibroblast

proliferation. A reason for this could be a dose dependant activity of the native protein that activates different phenotypical response switching cells between proliferation and migration. A study conducted by Donatis et al showed that PDGF at lower concentrations around 1 ng/ml promotes cell migration, whereas when the concentration rises above 5 ng/ml, it elicits a strong cell proliferation output [79]. This can be due to the fact that at lower PDGF concentrations, the receptor internalization is due to clatherin-mediated endocytosis, but at higher concentration it shifts to raft-mediated endocytosis which promotes mitosis of cells [79]. We use serum free media to check the activity of the individual proteins in *in vitro* assays without the effect of background growth factor. It would be interesting to study the effect of stressing the cells on the binding of protein ligand and receptor. A limitation of our studies performed was that we did not include a group that had ELP and PDGF-AA as separate proteins. It would be interesting to see how the cells react in presence of a combination of ELP nanoparticles and the growth factor.

ELP fused protein is more stable and has a longer half-life as compared to the native protein [72]. In conclusion, we synthesized PDGF A-ELP that has better or at least comparable biological activity to recombinant PDGF-AA. Based on previously conducted research using other ELP fused protein [48, 55], PDGF-ELP is expected to be more stable in the wound environment. The formation of self-assembling nanoparticles at physiological temperatures allows it to be used as a prospective drug delivery vehicle for chronic wound healing in diabetes [71] and spinal cord injury-induced pressure ulcers [75, 76] .

CHAPTER 7: FUTURE DIRECTIONS

The results obtained in the *in vitro* studies suggest certain ways in which the use of the fusion protein could be directed in the future:

- Stability studies of the native protein and the fusion protein in a human wound fluid with chronic conditions.
- Using ELP control at 5 nM concentration for tube assay to study its effect on capillary formation.
- *In vivo* studies: Using diabetic mice models to assess the activity of the nanoparticles *in vivo* would be one of the ways that would further strengthen our hypothesis that PDGF-ELP nanoparticles assist wound healing in chronic conditions like diabetes.
- Using a combination of growth factors to achieve even higher wound closure because the chronic wound environment is complex, hostile and requires the activity of several growth factor to achieve complete wound closure in time.
- Using a dermal scaffold as a delivery mechanism for the nanoparticles: Biomedical applications of tissue/dermal scaffolds have been widely studied [74]. The size of our nanoparticles is ~600-700 nm which is lesser than the pore size of most available dermal scaffolds (~1 μm). Incorporating our fusion protein with tissue scaffolds that already have proven effects on wound healing would be a good alternative to deliver our proteins.

REFERENCES

1. Richmond, N. A., Maderal, A. D., & Vivas, A. C. (2013). Evidence-based management of common chronic lower extremity ulcers. *Dermatologic therapy*, *26*(3), 187-196.
2. Frykberg, R. G., & Banks, J. (2015). Challenges in the Treatment of Chronic Wounds. Advances in wound care, 4(9), 560–582. doi:10.1089/wound.2015.0635
3. Boulton, A. J., Vileikyte, L., Ragnarson-Tennvall, G., & Apelqvist, J. (2005). The global burden of diabetic foot disease. *The Lancet*, *366*(9498), 1719-1724.
4. Alavi, A., Sibbald, R. G., Mayer, D., Goodman, L., Botros, M., Armstrong, D. G., ... & Kirsner, R. S. (2014). Diabetic foot ulcers: Part I. Pathophysiology and prevention. *Journal of the American Academy of Dermatology*, *70*(1), 1-e1.
5. Martins-Mendes, D., Monteiro-Soares, M., Boyko, E. J., Ribeiro, M., Barata, P., Lima, J., & Soares, R. (2014). The independent contribution of diabetic foot ulcer on lower extremity amputation and mortality risk. *Journal of Diabetes and its Complications*, *28*(5), 632-638.
6. Margolisa, D. J., Bilkerb, W., Santannab, J., & d Baumgartenc, M. (2002). Venous leg ulcer: incidence and prevalence in the elderly. *Journal of the American Academy of Dermatology*, *46*(3), 381-386.
7. Menke, N. B., Ward, K. R., Witten, T. M., Bonchev, D. G., & Diegelmann, R. F. (2007). Impaired wound healing. *Clinics in dermatology*, *25*(1), 19-25.
8. Gonzalez, A. C. D. O., Costa, T. F., Andrade, Z. D. A., & Medrado, A. R. A. P. (2016). Wound healing-A literature review. *Anais brasileiros de dermatologia*, *91*(5), 614-620.
9. Sorg, H., Tilkorn, D. J., Hager, S., Hauser, J., & Mirastschijski, U. (2017). Skin wound healing: an update on the current knowledge and concepts. European Surgical Research, 58(1-2), 81-94.
10. Singer, A. J., & Clark, R. A. (1999). Cutaneous wound healing. *New England journal of medicine*, *341*(10), 738-746.
11. Wysocki, A. B., Staiano-Coico, L., & Grinneill, F. (1993). Wound fluid from chronic leg ulcers contains elevated levels of metalloproteinases MMP-2 and MMP-9. *Journal of Investigative Dermatology*, *101*(1).
12. Gianino, E., Miller, C., & Gilmore, J. (2018). Smart Wound Dressings for Diabetic Chronic Wounds. *Bioengineering (Basel, Switzerland)*, *5*(3), 51. doi:10.3390/bioengineering5030051
13. Tandara, A. A., & Mustoe, T. A. (2004). Oxygen in wound healing—more than a nutrient. *World journal of surgery*, *28*(3), 294-300.
14. Guo, S., & Dipietro, L. A. (2010). Factors affecting wound healing. *Journal of dental research*, *89*(3), 219–229. doi:10.1177/0022034509359125
15. Harding, K. G., Morris, H. L., & Patel, G. K. (2002). Healing chronic wounds. *Bmj*, *324*(7330), 160-163.
16. Brem, H., Sheehan, P., & Boulton, A. J. (2004). Protocol for treatment of diabetic foot ulcers. *The American journal of surgery*, *187*(5), S1-S10.
17. Han, G., & Ceilley, R. (2017). Chronic Wound Healing: A Review of Current Management and Treatments. *Advances in therapy*, *34*(3), 599–610. doi:10.1007/s12325-017-0478-y

18. Murphy, P. S., & Evans, G. R. (2012). Advances in wound healing: a review of current wound healing products. *Plastic surgery international*, *2012*, 190436. doi:10.1155/2012/190436
19. Percival, S. L., Bowler, P., & Woods, E. J. (2008). Assessing the effect of an antimicrobial wound dressing on biofilms. *Wound repair and regeneration*, *16*(1), 52-57.
20. Yazdanpanah, L., Nasiri, M., & Adarvishi, S. (2015). Literature review on the management of diabetic foot ulcer. *World journal of diabetes*, *6*(1), 37–53. doi:10.4239/wjd.v6.i1.37
21. Falanga, V. (1992). Growth factors and chronic wounds: the need to understand the microenvironment. *The Journal of dermatology*, *19*(11), 667-672.
22. Barrientos, S., Stojadinovic, O., Golinko, M. S., Brem, H., & Tomic-Canic, M. (2008). Growth factors and cytokines in wound healing. *Wound repair and regeneration*, *16*(5), 585-601.
23. Shi, R., Lian, W., Han, S., Cao, C., Jin, Y., Yuan, Y., ... & Li, M. (2018). Nanosphere-mediated co-delivery of VEGF-A and PDGF-B genes for accelerating diabetic foot ulcers healing in rats. *Gene therapy*, *25*(6), 425-438.
24. Jee, J. P., Pangeni, R., Jha, S. K., Byun, Y., & Park, J. W. (2019). Preparation and in vivo evaluation of a topical hydrogel system incorporating highly skin-permeable growth factors, quercetin, and oxygen carriers for enhanced diabetic wound-healing therapy. *International Journal of Nanomedicine*, *14*, 5449.
25. Steed, D. L. (1995). Clinical evaluation of recombinant human platelet–derived growth factor for the treatment of lower extremity diabetic ulcers. *Journal of Vascular Surgery*, *21*(1), 71-81.
26. Fang, R. C., & Galiano, R. D. (2008). A review of becaplermin gel in the treatment of diabetic neuropathic foot ulcers. *Biologics : targets & therapy*, *2*(1), 1–12. doi:10.2147/btt.s1338
27. Antoniades, H. N., Scher, C. D., & Stiles, C. D. (1979). Purification of human platelet-derived growth factor. *Proceedings of the National Academy of Sciences*, *76*(4), 1809-1813.
28. Bennett, S. P., Griffiths, G. D., Schor, A. M., Leese, G. P., & Schor, S. L. (2003). Growth factors in the treatment of diabetic foot ulcers. *British Journal of Surgery*, *90*(2), 133-146.
29. Heldin, C. H., & Westermark, B. (1988). Role of platelet-derived growth factor in vivo. In *The molecular and cellular biology of wound repair* (pp. 249-273). Springer, Boston, MA.
30. Chen, P. H., Chen, X., & He, X. (2013). Platelet-derived growth factors and their receptors: structural and functional perspectives. *Biochimica et biophysica acta*, *1834*(10), 2176–2186. doi:10.1016/j.bbapap.2012.10.015
31. Battegay, E. J., Rupp, J., Iruela-Arispe, L., Sage, E. H., & Pech, M. (1994). PDGF-BB modulates endothelial proliferation and angiogenesis in vitro via PDGF beta-receptors. *The Journal of cell biology*, *125*(4), 917-928.
32. Lindahl, P., Johansson, B. R., Levéen, P., & Betsholtz, C. (1997). Pericyte loss and microaneurysm formation in PDGF-B-deficient mice. *Science*, *277*(5323), 242-245.

33. Stavri, G. T., Hong, Y., Zachary, I. C., Breier, G., Baskerville, P. A., Ylä-Herttuala, S., ... & Erusalimsky, J. D. (1995). Hypoxia and platelet-derived growth factor-BB synergistically upregulate the expression of vascular endothelial growth factor in vascular smooth muscle cells. *Febs Letters*, *358*(3), 311-315.
34. Lin, H., Chen, B., Sun, W., Zhao, W., Zhao, Y., & Dai, J. (2006). The effect of collagen-targeting platelet-derived growth factor on cellularization and vascularization of collagen scaffolds. *Biomaterials*, *27*(33), 5708-5714.
35. Pierce, G. F., Mustoe, T. A., Altrock, B. W., Deuel, T. F., & Thomason, A. (1991). Role of platelet-derived growth factor in wound healing. *Journal of cellular biochemistry*, *45*(4), 319-326.
36. Pierce, G. F., Mustoe, T. A., Senior, R. M., Reed, J., Griffin, G. L., Thomason, A., & Deuel, T. F. (1988). In vivo incisional wound healing augmented by platelet-derived growth factor and recombinant c-sis gene homodimeric proteins. *The Journal of experimental medicine*, *167*(3), 974-987.
37. Greenhalgh, D. G., Sprugel, K. H., Murray, M. J., & Ross, R. (1990). PDGF and FGF stimulate wound healing in the genetically diabetic mouse. *The American journal of pathology*, *136*(6), 1235.
38. Fang, R. C., & Galiano, R. D. (2008). A review of becaplermin gel in the treatment of diabetic neuropathic foot ulcers. *Biologics : targets & therapy*, *2*(1), 1–12. doi:10.2147/btt.s1338
39. Steed, D. L. (1995). Clinical evaluation of recombinant human platelet–derived growth factor for the treatment of lower extremity diabetic ulcers. *Journal of Vascular Surgery*, *21*(1), 71-81.
40. Wieman, T. J., Smiell, J. M., & Su, Y. (1998). Efficacy and safely of a topical gel formulation of recombinant human platelet-derived growth factor-BB (becaplermin) in patients with chronic neuropathic diabetic ulcers: a phase III randomized placebo-controlled double-blind study. *Diabetes care*, *21*(5), 822-827.
41. Smiell, J. M., Wieman, T. J., Steed, D. L., Perry, B. H., Sampson, A. R., & Schwab, B. H. (1999). Efficacy and safety of becaplermin (recombinant human platelet-derived growth factor-BB) in patients with nonhealing, lower extremity diabetic ulcers: a combined analysis of four randomized studies. *Wound Repair and Regeneration*, *7*(5), 335-346.
42. Mast, B. A., & Schultz, G. S. (1996). Interactions of cytokines, growth factors, and proteases in acute and chronic wounds. *Wound Repair and Regeneration*, *4*(4), 411-420.
43. Chen, R. R., & Mooney, D. J. (2003). Polymeric growth factor delivery strategies for tissue engineering. *Pharmaceutical research*, *20*(8), 1103-1112.
44. Pietras, K., Sjöblom, T., Rubin, K., Heldin, C. H., & Östman, A. (2003). PDGF receptors as cancer drug targets. *Cancer cell*, *3*(5), 439-443.
45. Moustakas, A., & Heldin, C. H. (2016). Mechanisms of TGFβ-induced epithelial–mesenchymal transition. *Journal of clinical medicine*, *5*(7), 63.
46. https://www.fda.gov/media/76010/download
47. Shamji, M. F., Betre, H., Kraus, V. B., Chen, J., Chilkoti, A., Pichika, R., ... & Setton, L. A. (2007). Development and characterization of a fusion protein between thermally responsive elastin-like polypeptide and interleukin-1 receptor antagonist: Sustained

release of a local antiinflammatory therapeutic. *Arthritis & Rheumatism: Official Journal of the American College of Rheumatology*, *56*(11), 3650-3661.

48. Koria, P., Yagi, H., Kitagawa, Y., Megeed, Z., Nahmias, Y., Sheridan, R., & Yarmush, M. L. (2011). Self-assembling elastin-like peptides growth factor chimeric nanoparticles for the treatment of chronic wounds. *Proceedings of the National Academy of Sciences*, *108*(3), 1034-1039.
49. Hassouneh, W., Christensen, T., & Chilkoti, A. (2010). Elastin-like polypeptides as a purification tag for recombinant proteins. *Current protocols in protein science*, *Chapter 6*, Unit–6.11. doi:10.1002/0471140864.ps0611s61
50. Meyer, D. E., & Chilkoti, A. (1999). Purification of recombinant proteins by fusion with thermally-responsive polypeptides. *Nature biotechnology*, *17*(11), 1112-1115.
51. Shamji, M. F., Betre, H., Kraus, V. B., Chen, J., Chilkoti, A., Pichika, R., ... & Setton, L. A. (2007). Development and characterization of a fusion protein between thermally responsive elastin-like polypeptide and interleukin-1 receptor antagonist: Sustained release of a local antiinflammatory therapeutic. *Arthritis & Rheumatism: Official Journal of the American College of Rheumatology*, *56*(11), 3650-3661.
52. Amiram, M., Luginbuhl, K. M., Li, X., Feinglos, M. N., & Chilkoti, A. (2013). A depot-forming glucagon-like peptide-1 fusion protein reduces blood glucose for five days with a single injection. *Journal of controlled release*, *172*(1), 144-151.
53. Senior, R. M., Griffin, G. L., Mecham, R. P., Wrenn, D. S., Prasad, K. U., & Urry, D. W. (1984). Val-Gly-Val-Ala-Pro-Gly, a repeating peptide in elastin, is chemotactic for fibroblasts and monocytes. *The Journal of cell biology*, *99*(3), 870-874.
54. Kamoun, A., Landeau, J. M., Godeau, G., Wallach, J., Duchesnay, A., Pellat, B., & Hornebeck, W. (1995). Growth stimulation of human skin fibroblasts by elastin-derived peptides. *Cell adhesion and communication*, *3*(4), 273-281.
55. Yeboah, A., Cohen, R. I., Rabolli, C., Yarmush, M. L., & Berthiaume, F. (2016). Elastin-like polypeptides: A strategic fusion partner for biologics. *Biotechnology and bioengineering*, *113*(8), 1617-1627.
56. Peus, D., Jungtäubl, H., Knaub, S., Leuker, A., Gerecht, K., Ostendorf, R., ... & Scharffetter-Kochanek, K. (1995). Localization of platelet-derived growth factor receptor subunit expression in chronic venous leg ulcers: Young investigator award. *Wound Repair and Regeneration*, *3*(3), 265-272.
57. Ågren, M. S., Steenfos, H. H., Dabelsteen, S., Hansen, J. B., & Dabelsteen, E. (1999). Proliferation and mitogenic response to PDGF-BB of fibroblasts isolated from chronic venous leg ulcers is ulcer-age dependent. *Journal of Investigative Dermatology*, *112*(4), 463-469.
58. Yu, J., Moon, A., & Kim, H. R. C. (2001). Both platelet-derived growth factor receptor (PDGFR)-α and PDGFR-β promote murine fibroblast cell migration. *Biochemical and biophysical research communications*, *282*(3), 697-700.
59. Pierce, G. F., Tarpley, J. E., Allman, R. M., Goode, P. S., Serdar, C. M., Morris, B., ... & Berg, J. V. (1994). Tissue repair processes in healing chronic pressure ulcers treated with recombinant platelet-derived growth factor BB. *The American journal of pathology*, *145*(6), 1399.

60. Zetter, B. R., & Antoniades, H. N. (1979). Stimulation of human vascular endothelial cell growth by a platelet-derived growth factor and thrombin. *Journal of supramolecular structure*, *11*(3), 361-370.
61. Wang, Y., Pennock, S. D., Chen, X., Kazlauskas, A., & Wang, Z. (2004). Platelet-derived growth factor receptor-mediated signal transduction from endosomes. *Journal of Biological Chemistry*, *279*(9), 8038-8046.
62. Kawada, K., Upadhyay, G., Ferandon, S., Janarthanan, S., Hall, M., Vilardaga, J. P., & Yajnik, V. (2009). Cell migration is regulated by platelet-derived growth factor receptor endocytosis. *Molecular and cellular biology*, *29*(16), 4508-4518.
63. Seppä, H., Grotendorst, G., Seppä, S., Schiffmann, E., & Martin, G. R. (1982). Platelet-derived growth factor in chemotactic for fibroblasts. The Journal of cell biology, 92(2), 584-588.
64. Piran, M., Vakilian, S., Piran, M., Mohammadi-Sangcheshmeh, A., Hosseinzadeh, S., & Ardeshirylajimi, A. (2018). In vitro fibroblast migration by sustained release of PDGF-BB loaded in chitosan nanoparticles incorporated in electrospun nanofibers for wound dressing applications. *Artificial cells, nanomedicine, and biotechnology*, *46*(sup1), 511-520.
65. Liang, C. C., Park, A. Y., & Guan, J. L. (2007). In vitro scratch assay: a convenient and inexpensive method for analysis of cell migration in vitro. *Nature protocols*, *2*(2), 329.
66. Risau, W., Drexler, H., Mironov, V., Smits, A., Siegbahn, A., Funa, K., & Heldin, C. H. (1992). Platelet-derived growth factor is angiogenic in vivo. *Growth factors*, *7*(4), 261-266.
67. Sato, N., Beitz, J. G., Kato, J., Yamamoto, M., Clark, J. W., Calabresi, P., Raymond, A., & Frackelton, A. R., Jr (1993). Platelet-derived growth factor indirectly stimulates angiogenesis in vitro. *The American journal of pathology*, *142*(4), 1119–1130.
68. Li, H., Fu, X., Zhang, L., Huang, Q., Wu, Z., & Sun, T. (2008). Research of PDGF-BB gel on the wound healing of diabetic rats and its pharmacodynamics. *Journal of Surgical Research*, *145*(1), 41-48.
69. Carmeliet, P., & Jain, R. K. (2011). Molecular mechanisms and clinical applications of angiogenesis. *Nature*, *473*(7347), 298-307.
70. DeCicco-Skinner, K. L., Henry, G. H., Cataisson, C., Tabib, T., Gwilliam, J. C., Watson, N. J., Bullwinkle, E. M., Falkenburg, L., O'Neill, R. C., Morin, A., & Wiest, J. S. (2014). Endothelial cell tube formation assay for the in vitro study of angiogenesis. *Journal of visualized experiments : JoVE*, (91), e51312. https://doi.org/10.3791/51312
71. Sen, C. K. (2019). Human wounds and its burden: an updated compendium of estimates.
72. Floss, D. M., Conrad, U., Rose-John, S., & Scheller, J. (2013). Fusion protein technologies for biopharmaceuticals: applications and challenges.
73. Yeboah, A., Cohen, R. I., Faulknor, R., Schloss, R., Yarmush, M. L., & Berthiaume, F. (2016). The development and characterization of SDF1α-elastin-like-peptide nanoparticles for wound healing. *Journal of Controlled Release*, *232*, 238-247.
74. Rahmani Del Bakhshayesh, A., Annabi, N., Khalilov, R., Akbarzadeh, A., Samiei, M., Alizadeh, E., ... & Montaseri, A. (2018). Recent advances on biomedical applications of scaffolds in wound healing and dermal tissue engineering. *Artificial cells, nanomedicine, and biotechnology*, *46*(4), 691-705.

75. Kumar, S., Tan, Y., Yarmush, M. L., Dash, B. C., Hsia, H. C., & Berthiaume, F. (2019). Mouse Model of Pressure Ulcers After Spinal Cord Injury. *JoVE (Journal of Visualized Experiments)*, (145), e58188.
76. Kumar, S., Yarmush, M. L., Dash, B. C., Hsia, H. C., & Berthiaume, F. (2018). Impact of complete spinal cord injury on healing of skin ulcers in mouse models. *Journal of neurotrauma*, *35*(6), 815-824.
77. Hughes, J. M., Budd, P. M., Tiede, K., & Lewis, J. (2015). Polymerized high internal phase emulsion monoliths for the chromatographic separation of engineered nanoparticles. *Journal of Applied Polymer Science*, *132*(1).
78. Kowalczyk, T., Hnatuszko-Konka, K., Gerszberg, A., & Kononowicz, A. K. (2014). Elastin-like polypeptides as a promising family of genetically-engineered protein based polymers. *World journal of microbiology & biotechnology*, *30*(8), 2141–2152. https://doi.org/10.1007/s11274-014-1649-5
79. De Donatis, A., Comito, G., Buricchi, F., Vinci, M. C., Parenti, A., Caselli, A., ... & Cirri, P. (2008). Proliferation versus migration in platelet-derived growth factor signaling the key role of endocytosis. *Journal of Biological Chemistry*, *283*(29), 19948-19956.
80. https://www.essenbioscience.com/en/protocols/incucyte-cell-count-proliferation-assay-general-pr/
81. https://www.essenbioscience.com/en/applications/live-cell-assays/scratch-wound-cell-migration-invasion/